Journal of Applied Mathematics and Computing
https://doi.org/10.1007/s12190-023-01877-5

ORIGINAL RESEARCH

Check for updates

Dynamics of a fractional COVID-19 model with immunity using harmonic incidence mean-type

Nandhini Mohankumar[1] · Lavanya Rajagopal[1]

Received: 11 January 2023 / Revised: 28 March 2023 / Accepted: 7 May 2023

Abstract
The transmission dynamics of COVID-19 is investigated through the prism of the Atangana-Baleanu fractional model with acquired immunity. Harmonic incidence mean-type aims to drive exposed and infected populations towards extinction in a finite time frame. The reproduction number is calculated based on the next-generation matrix. A disease-free equilibrium point can be achieved globally using the Castillo-Chavez approach. Using the additive compound matrix approach, the global stability of endemic equilibrium can be demonstrated. Utilizing Pontryagin's maximum principle, we introduce three control variables to obtain the optimal control strategies. Laplace transform allows simulating the fractional-order derivatives analytically. Analysis of the graphical results led to a better understanding of the transmission dynamics.

Keywords COVID-19 · Reproduction number · Immunity · Harmonic incidence mean-type

Mathematics Subject Classification 34A08 · 34D23 · 49K15

1 Introduction

The global SARS-CoV-2 pandemic caused substantial death tolls, along with significant economic and personal damage. Despite the widespread transmission of the

R. Lavanya author contributed equally to this work.

✉ Lavanya Rajagopal
lavnya.gopal@gmail.com

Nandhini Mohankumar
nandhinimohankumar@gmail.com

[1] Department of Mathematics, Coimbatore Institute of Technology, Civil Aerodrome (PO), Coimbatore, Tamilnadu 641014, India

Published online: 31 May 2023

Journal of Applied Nonlinear Dynamics

http://lhscientificpublishing.com/Journals/JAND-Default.aspx

A Study on Optimal Control of a COVID-19 Transmission Model with the Significance of Early Screening and Testing Measures

Natedhini Mohankumar[1], Lavanya Rajagopal

Department of Mathematics, Coimbatore Institute of Technology, Tamilnadu, India

Submission Info

Communicated by Jorge Duarte
Received 15 December 2021
Accepted 23 January 2022
Available online 1 July 2023

Keywords

Corona virus
Mathematical modeling
Stability
Optimal control

Abstract

In this paper, we present a deterministic *SEQIR* mathematical model that describes the transmission dynamics of COVID-19 that also includes testing procedures in the quarantine stage. The reproduction number R_0 is derived with some properties of the model. The stability of equilibrium points is analyzed. An objective function is proposed and optimal control strategies are derived using Pontryagin's Maximum Principle. The existence and uniqueness of an optimality system are demonstrated. Numerical simulations are presented in different scenarios with the control interventions early screening, prevention measures of COVID-19, and following a healthy lifestyle. The main objective of the paper is to eradicate the disease in exposed stage. The chosen control variables helps us to reduce the exposed population.

1 Introduction

The SARS Coronavirus or SARS-CoV-2 has swept the globe since the virus emerged in Wuhan City, China [1]. As of December 2019, numerous people in China have been diagnosed with severe pneumonia. Many patients had the same exposure from the Huanan seafood market. World Health Organization (WHO) received notification of the outbreak in Wuhan because of the increasing number of infected persons [2]. From January 1st, 2020 to January 31st, 2020, COVID-19 infections have spread internationally by the massive migration of Chinese people during the Chinese New Year. COVID-19 infections are confirmed to have spread between humans outside of China. As a result, those who had never been to China acquired the disease from locals [3]. The COVID-19 outbreak is an unfortunate disaster affecting social, economic, and health factors worldwide.

In the COVID-19 outbreak, managing severe patients has become a challenging issue because of the rapid increase in newly confirmed and severe cases. With no ready access to diagnostic tools and without the sustainability of healthcare systems to handle the outbreak, health service providers had difficulty making rapid decisions about SARS-Cov-2 transmission rate. Amid the COVID-19 pandemic, health care providers have observed an increasing number of patients who delay or skip preventive screenings

[1]Corresponding author.
Email address: lavnya.gopal@gmail.com

ISSN 2164-6457, eISSN 2164-6473/$-see front materials
DOI:10.5890/JAND.2023.09.005

AIMS Mathematical Biosciences and Engineering

http://www.aimspress.com/journal/mbe

MBE, 20(6): 9861–9875.
DOI: 10.3934/mbe.2023432
Received: 25 January 2023
Revised: 06 March 2023
Accepted: 12 March 2023
Published: 24 March 2023

Research article

Optimal control for co-infection with COVID-19-Associated Pulmonary Aspergillosis in ICU patients with environmental contamination

Nandhini Mohankumar[1], Lavanya Rajagopal[1] and Juan J. Nieto[2,*]

[1] Department of Mathematics, Coimbatore Institute of Technology, Tamilnadu, India

[2] CITMAga, Departamento de Estatística, Análise Matemática e Optimización, Universidade de Santiago de Compostela, 15782 Santiago de Compostela, Spain

* **Correspondence:** Email: juanjose.nieto.roig@usc.es.

Abstract: In this paper, we propose a mathematical model for COVID-19-Associated Pulmonary Aspergillosis (CAPA) co-infection, that enables the study of relationship between prevention and treatment. The next generation matrix is employed to find the reproduction number. We enhanced the co-infection model by incorporating time-dependent controls as interventions based on Pontryagin's maximum principle in obtaining the necessary conditions for optimal control. Finally, we perform numerical experiments with different control groups to assess the elimination of infection. In numerical results, transmission prevention control, treatment controls, and environmental disinfection control provide the best chance of preventing the spread of diseases more rapidly than any other combination of controls.

Keywords: co-infection; CAPA; hospital environment; reproduction number; optimal control

1. Introduction

The world is in the grip of a pandemic triggered by SARS-CoV-2, which has infected more than 24 million people with a mortality rate exceeding 3 percent. There weren't many reports of super infections during the early stages of the current pandemic, but now they seem to be occurring more frequently, specifically secondary fungal diseases [1]. Patients with COVID-19 have been diagnosed with viral, bacterial, and fungal co-infections. Early detection of these co-infections is crucial to implementing an effective antimicrobial regime [2]. COVID-19 patients have suffered from several fatal complications. Invasive pulmonary aspergillosis (IPA) was associated with a poor prognosis, particularly among those experiencing acute respiratory distress syndrome (ARDS) in intensive care units [3].

According to reports, 19 to 35 percent of COVID-19 patients have co-infection with Aspergillus. As

axioms

MDPI

Article

A Fractional COVID-19 Model with Efficacy of Vaccination

M. Nandhini [1], R. Lavanya [1] and Juan J. Nieto [2,*]

[1] Department of Mathematics, Coimbatore Institute of Technology, Coimbatore 641014, Tamil Nadu, India
[2] CITMAga, Departamento de Estatística, Análise Matemática e Optimización, Universidade de Santiago de Compostela, 15782 Santiago de Compostela, Spain
* Correspondence: juanjose.nieto.roig@usc.es

Abstract: This paper develops a fractional-order model of COVID-19 with vaccination. The model is well designed by including both the efficacy and inefficacy of vaccinations in humans. Besides calculating the reproduction number, equilibrium points and the feasibility region are also determined. Stability analysis for the proposed model around equilibrium points is discussed. Fixed-point theory is employed to identify the singularity of the solution. Adomian decomposition and Laplace integral transformation are combined to obtain the solution. We present the solutions graphically to analyze the contributions of the disease dynamics based on different values of the fractional order. This study seeks an in-depth understanding of COVID-19 transmission to improve health outcomes.

Keywords: COVID-19; reproduction number; fractional mathematical model; fixed point

AMS Classification: 34A08; 34D20; 65P99

1. Introduction

The World Health Organization issued a public health emergency of international concern on 30 January 2020 and a pandemic alert in March 2020 in response to the rapid and extensive spread of Coronavirus Disease 2019. Initially, the disease turned out to be an epidemic in mainland China first hitting Wuhan, in the province of Hubei [1]. India had the second-highest confirmed cases in the world. The direct transmission of SARS-CoV-2 was conclusively proven by clinical evidence in January 2020 [2]. Four consecutive lockdowns came into effect in India as a preventive measure. In the absence of vaccines, social distancing serves as the best control measure against COVID-19 [3].

As a part of the vaccination program, India has established a NEGVAC (National Expert Group on Vaccine Administration for COVID-19) committee to develop guidelines for the COVID-19 vaccine administration [4]. There have been vaccination campaigns conducted around the world to combat COVID-19. Several types of vaccines are available for COVID-19 [5]. Furthermore, India has exported 35,793,000 doses of vaccine internationally (commercial exports). Innovative technologies are tested during the development of vaccines to determine if they work. Vaccine development, which is dependent on public approval, determines the effectiveness of the vaccination program based on perception and beliefs surrounding the vaccine [6]. In addition, a significant portion of the population remains uncertain about the vaccine. The perception of the vaccine among people may change with the advent of awareness programs and the improvement of vaccine outcomes [7].

Fractional-order differential equations are the most effective tool for studying biological and engineering systems. Several fractional-order derivatives comprise numerical models of physical and biological systems [8,9]. There are numerous motivations to employ fractional order, but the main focus is on dealing with the memory dynamics evident in many biological systems. Differential equations derived using the fractional derivative have several applications to analyze various infectious disease transmission dynamics such as HIV/AIDS, TB, and others [10].

check for updates

Citation: Nandhini, M.; Lavanya, R.; Nieto, J.J. A Fractional COVID-19 Model with Efficacy of Vaccination. *Axioms* **2022**, *11*, 446. https://doi.org/10.3390/axioms11090446

Academic Editor: Hans J. Haubold

Received: 1 August 2022
Accepted: 26 August 2022
Published: 31 August 2022

Publisher's Note: MDPI stays neutral with regard to jurisdictional claims in published maps and institutional affiliations.

Proyecciones Journal of Mathematics
Vol. 41, N° 4, pp. 879-890, August 2022.
Universidad Católica del Norte
Antofagasta - Chile

10.22199/issn.0717-6279-4475

Minimal connected restrained monophonic sets in graphs

A. P. Santhakumaran,
Hindustan Institute of Technology and Science, India
P. Titus
University College of Engineering Nagercoil, India
and
K. Ganesamoorthy *
Coimbatore Institute of Technology, India
Received : September 2021. Accepted : February 2022

Abstract

For a connected graph $G = (V, E)$ of order at least two, a connected restrained monophonic set S of G is a restrained monophonic set such that the subgraph $G[S]$ induced by S is connected. The minimum cardinality of a connected restrained monophonic set of G is the connected restrained monophonic number of G and is denoted by $m_{cr}(G)$. A connected restrained monophonic set S of G is called a minimal connected restrained monophonic set if no proper subset of S is a connected restrained monophonic set of G. The upper connected restrained monophonic number of G, denoted by $m^+_{cr}(G)$, is defined as the maximum cardinality of a minimal connected restrained monophonic set of G. We determine bounds for it and certain general properties satisfied by this parameter are studied. It is shown that, for positive integers a, b such that $4 \leq a \leq b$, there exists a connected graph G such that $m_{cr}(G) = a$ and $m^+_{cr}(G) = b$.

Key Words: *restrained monophonic set, restrained monophonic number, connected restrained monophonic set, connected restrained monophonic number, minimal connected restrained monophonic set.*

AMS Subject Classification: *05C12.*

Научный отдел

МАТЕМАТИКА

Известия Саратовского университета. Новая серия. Серия: Математика. Механика. Информатика. 2022. Т. 22, вып. 3. С. 278–286
Izvestiya of Saratov University. Mathematics. Mechanics. Informatics, 2022, vol. 22, iss. 3, pp. 278–286
mmi.sgu.ru
https://doi.org/10.18500/1816-9791-2022-22-3-278-286
EDN: IMTPKR

Article

Forcing total outer connected monophonic number of a graph

K. Ganesamoorthy[1]✉, **S. Lakshmi Priya**[2]

[1]Coimbatore Institute of Technology, Department of Mathematics, Coimbatore — 641 014, India
[2]CIT Sandwich Polytechnic College, Department of Mathematics, Coimbatore — 641 014, India
Kathiresan Ganesamoorthy, kvgm_2005@yahoo.co.in, https://orcid.org/0000-0003-2769-1991
Shanmugam Lakshmi Priya, lakshmiuspriya@gmail.com, https://orcid.org/0000-0001-7367-1532

Abstract. For a connected graph $G = (V, E)$ of order at least two, a subset T of a minimum total outer connected monophonic set S of G is a *forcing total outer connected monophonic subset* for S if S is the unique minimum total outer connected monophonic set containing T. A forcing total outer connected monophonic subset for S of minimum cardinality is a *minimum forcing total outer connected monophonic subset* of S. The *forcing total outer connected monophonic number* $f_{tom}(S)$ in G is the cardinality of a minimum forcing total outer connected monophonic subset of S. The *forcing total outer connected monophonic number* of G is $f_{tom}(G) = \min\{f_{tom}(S)\}$, where the minimum is taken over all minimum total outer connected monophonic sets S in G. We determine bounds for it and find the forcing total outer connected monophonic number of a certain class of graphs. It is shown that for every pair a, b of positive integers with $0 \leqslant a < b$ and $b \geqslant a + 4$, there exists a connected graph G such that $f_{tom}(G) = a$ and $cm_{to}(G) = b$, where $cm_{to}(G)$ is the total outer connected monophonic number of a graph.

Keywords: total outer connected monophonic set, total outer connected monophonic number, forcing total outer connected monophonic subset, forcing total outer connected monophonic number

Discrete Mathematics, Algorithms and Applications | Vol. 15, No. 05, 2250128 (2023)

| Research Paper

No Access

More on the outer connected geodetic number of a graph

K. Ganesamoorthy and D. Jayanthi

https://doi.org/10.1142/S1793830922501282 | Cited by: 1

< Previous Next >

Abstract

For a connected graph $G = (V, E)$ of order at least two, a *total outer connected geodetic set* S of a graph G is an outer connected geodetic set such that the subgraph induced by S has no isolated vertices. The minimum cardinality of a total outer connected geodetic set of G is the *total outer connected geodetic number* of G and is

INTERNATIONAL JOURNAL OF COMPUTER MATHEMATICS: COMPUTER SYSTEMS THEORY
2022, VOL. 7, NO. 2, 139–148
https://doi.org/10.1080/23799927.2022.2071765

On the connected monophonic number of a graph

K. Ganesamoorthy[a], M. Murugan[a] and A. P. Santhakumaran[b,†]

[a]Department of Mathematics, Coimbatore Institute of Technology, Coimbatore, India; [b]Department of Mathematics, Hindustan Institute of Technology and Science, Chennai, India

ABSTRACT

For a connected graph G of order at least two, a *connected monophonic set* of G is a monophonic set S such that the subgraph $G[S]$ induced by S is connected. The minimum cardinality of a connected monophonic set of G is the *connected monophonic number* of G and is denoted by $m_c(G)$. The number of extreme vertices and cut-vertices of G is its *extreme-cut order* $ec(G)$. A graph G is an *extreme-cut connected monophonic graph* if $m_c(G) = ec(G)$. Some interesting results on the extreme-cut connected monophonic graphs G are studied. For positive integers r, d and $k \geq 5$ with $r < d$, there exists an extreme-cut connected monophonic graph G with monophonic radius r, monophonic diameter d and the connected monophonic number k. Also if p, d and k are positive integers such that $2 \leq d \leq k-3$ and $p - d + k \geq 0$, then there exists an extreme-cut connected monophonic graph G of order p with monophonic diameter d and $m_c(G) = k$.

ARTICLE HISTORY
Received 14 September 2021
Revised 8 March 2022
Accepted 15 April 2022

KEYWORDS
Connected monophonic set; connected monophonic number; extreme-cut order; extreme-cut connected monophonic graph

AMS SUBJECT CLASSIFICATION
05C12

1. Introduction

Graph $G = (V, E)$ is a finite undirected connected graph without loops or multiple edges. The *order* and *size* of G are denoted by p and q, respectively. For basic graph theoretic terminology we refer to Harary [1,7]. A *u–v path* is an alternating sequence of vertices and edges: $u = v_0, e_1, v_1, e_2, v_2, \ldots, e_n, v_n = v$ such that $v_{i-1}v_i (1 \leq i \leq n)$ is an edge with all the vertices being distinct. For any two vertices u and v in G, the *distance* $d(u, v)$ is the length of a shortest u–v path in G. An u–v path of length $d(u, v)$ is called *u–v geodesic*. A maximal connected subgraph of G is called a *component* of G. A *cut-vertex* of a graph is one whose removal increases the number of components of G. The *neighborhood* of a vertex v is the set $N(v)$ consisting of all vertices u which are adjacent with v. A vertex v is an *extreme vertex* if the subgraph induced by its neighbors is complete. The number of extreme vertices and cut-vertices of G is its *extreme-cut order* $ec(G)$. A vertex v of G is called an *endvertex* of G if its degree is 1. A vertex v of G is called a *support vertex* of G if it is adjacent to an endvertex of G. The number of extreme vertices and support vertices of G is its *extreme-support orderes*(G).

A *chord* of a path P is an edge joining two non-adjacent vertices of P. A path P is called a *monophonic path* if it is a chordless path. A set S of vertices of G is a *monophonic set* of G if each vertex v of G lies on a x–y monophonic path for some x and y in S. The minimum cardinality of a monophonic set of G is the *monophonic number* of G and is denoted by $m(G)$. The monophonic number of a graph was studied and discussed in [2–4,8,11,12,14]. A *connected monophonic set* of G is a monophonic set S such

CONTACT K. Ganesamoorthy kvgm_2005@yahoo.co.in Department of Mathematics, Coimbatore Institute of Technology, Coimbatore 641 014, India
†Former Professor

COMMUNICATIONS IN COMBINATORICS AND OPTIMIZATION
Vol. 7, No. 2 (2022), pp.211-226
DOI: 10.22049/CCO.2021.27042.1184

CCO
COMMUN. COMB. OPTIM.

Research Article

Extreme outer connected monophonic graphs

K. Ganesamoorthy[†], S. Lakshmi Priya[*]

Department of Mathematics, Coimbatore Institute of Technology, Coimbatore - 641 014, India
[†]kvgm_2005@yahoo.co.in
[*]lakshmiuspriya@gmail.com

Received: 9 December 2020; Accepted: 26 July 2021
Published Online: 28 July 2021

Abstract: For a connected graph G of order at least two, a set S of vertices in a graph G is said to be an *outer connected monophonic set* if S is a monophonic set of G and either $S = V$ or the subgraph induced by $V - S$ is connected. The minimum cardinality of an outer connected monophonic set of G is the *outer connected monophonic number* of G and is denoted by $m_{oc}(G)$. The number of extreme vertices in G is its *extreme order* $ex(G)$. A graph G is said to be an *extreme outer connected monophonic graph* if $m_{oc}(G) = ex(G)$. Extreme outer connected monophonic graphs of order p with outer connected monophonic number p and extreme outer connected monophonic graphs of order p with outer connected monophonic number $p - 1$ are characterized. It is shown that for every pair a, b of integers with $0 \leq a \leq b$ and $b \geq 2$, there exists a connected graph G with $ex(G) = a$ and $m_{oc}(G) = b$. Also, it is shown that for positive integers r, d and $k \geq 2$ with $r < d$, there exists an extreme outer connected monophonic graph G with monophonic radius r, monophonic diameter d and outer connected monophonic number k.

Keywords: outer connected monophonic set, outer connected monophonic number, extreme order, extreme outer connected monophonic graph

AMS Subject classification: 05C12

1. Introduction

By a graph $G = (V, E)$ we mean a finite simple undirected connected graph. The order and size of G are denoted by p and q, respectively. For basic graph theoretic terminology we refer to Harary [5, 15]. The *distance* $d(x, y)$ between two vertices x and y in G is the length of a shortest $x - y$ path in G. A $x - y$ path of length $d(x, y)$ is called $x - y$ *geodesic*. The removal of a vertex v from a graph G results

[*] *Corresponding Author*

Hindawi
Journal of Nanomaterials
Volume 2022, Article ID 1865763, 17 pages
https://doi.org/10.1155/2022/1865763

Research Article

Thermal Radiation and Viscous Dissipation Impacts of Water and Kerosene-Based Carbon Nanotubes over a Heated Riga Sheet

R. Prabakaran,[1] **S. Eswaramoorthi**,[2] **K. Loganathan**,[3] **and Sonam Gyeltshen**[4]

[1]*Department of Mathematics, Coimbatore Institute of Technology, Coimbatore, 641014 Tamil Nadu, India*
[2]*Department of Mathematics, Dr. N.G.P. Arts and Science College, Coimbatore, 641048 Tamil Nadu, India*
[3]*Department of Mathematics and Statistics, Manipal University Jaipur, Jaipur, 303007 Rajasthan, India*
[4]*Department of Humanities and Management, Jigme Namgyel Engineering College, Royal University of Bhutan, Dewathang, Bhutan*

Correspondence should be addressed to S. Eswaramoorthi; eswaran.bharathiar@gmail.com and Sonam Gyeltshen; sonamgyeltshen@jnec.edu.bt

Received 16 July 2022; Revised 12 September 2022; Accepted 15 September 2022; Published 3 October 2022

Academic Editor: Bhanu P. Singh

This research communication explains the flow of water/kerosene-based CNTs (carbon nanotubes) over a Riga sheet. The energy analysis is debated with the availability of radiation, viscous dissipation, and convective heating conditions. Two divisions of CNTs, like, SWCNTs (single-wall carbon nanotubes) and MWCNTs (multiwall carbon nanotubes), are considered. The pertinent variables are applied to overhaul the governing mathematical models into ODE expressions. The overhaul expressions are analytically solved by HAM (homotopy analysis method) and numerically solved by MATLAB bvp4c scheme. The repercussions of relevant parameters on nanoliquid velocity, nanoliquid temperature, skin friction coefficient, and local Nusselt number are inspected via graphs, tables, and charts. Our computational results are compared with the previous researcher results and have the most acceptable agreement. Our outcomes are used to understand the flow attributes, behavior, and how to predict it for those working in the design of thermal equipment in thermal industry. It is noticed that the nanoliquid velocity decayed in counter to the unsteady parameter, and it enhances for larger values of Hartmann number. The nanoliquid temperature enriches when raising the Biot number and radiation parameter. The change in unsteady parameter decays the surface shear stress, while reverse results are found in the local Nusselt number.

1. Introduction

In recent decades, enhancing the rate of liquid thermal transport in classical base liquids (engine oil, water, polymer-based solutions) has been a crucial challenge for modern researchers and technologists. One approach to enrich the liquid thermal conductivity is to mix nanometer size metallic particles (carbides, fullerene, oxides, nitrides, metals, and carbon nanotubes) with the classical base liquids. Carbon nanotubes are cylindrical format tubes with precious attributes such as robust thermal conductivity and enormous energy. These CNTs are segregated into SWCNTs (single-wall carbon nanotubes) and MWCNTs (multiwall carbon nanotubes) and are highly used in many industrial processes, like, drug delivery, nanotube transistors, microwave amplifiers, pancreatic cancer test, and optics. Haq et al. [1] noted that the higher surface shear stress attains in engine oil-based CNTs compared to ethylene glycol-based CNTs in their MHD flow of CNTs over a stretching surface. The consequences of gasoline oil-based hybrid CNTs past a curved stretched surface by Muhammad et al. [2], and noticed that the nanoliquid velocity enhances for enriching both CNTs volume fractions. Gholinia et al. [3] proved that the nanoliquid temperature for SWCNTs is larger than the MWCNTs for the problem of the 3D flow of hybrid nanoliquids on a cylinder. They utilize ethylene glycol, water, and engine oil which are the base fluids. The 3D flow of carbon nanotubes past a variable ticked stretching surface was employed by Imtiaz et al. [4]. They concluded that the nanoliquid flow improves when increasing

micromachines

MDPI

Article

Investigation on Thermally Radiative Mixed Convective Flow of Carbon Nanotubes/Al_2O_3 Nanofluid in Water Past a Stretching Plate with Joule Heating and Viscous Dissipation

R. Prabakaran [1], S. Eswaramoorthi [2,*], Karuppusamy Loganathan [3,4] and Ioannis E. Sarris [5,*]

[1] Department of Mathematics, Coimbatore Institute of Technology, Coimbatore 641014, Tamil Nadu, India
[2] Department of Mathematics, Dr. N.G.P. Arts and Science College, Coimbatore 641048, Tamil Nadu, India
[3] Department of Mathematics and Statistics, Manipal University Jaipur, Jaipur 303007, Rajasthan, India
[4] Research and Development Wing, Live4Research, Tiruppur 638106, Tamil Nadu, India
[5] Department of Mechanical Engineering, University of West Attica, 12244 Athens, Greece
* Correspondence: eswaran.bharathiar@gmail.com (S.E.); sarris@uniwa.gr (I.E.S.)

Abstract: The nature of this prevailing inquisition is to scrutinize the repercussion of MHD mixed convective flow of CNTs/Al_2O_3 nanofluid in water past a heated stretchy plate with injection/suction, heat consumption and radiation. The Joule heating and viscous dissipation are included in our investigation. The Navier–Stokes equations are implemented to frame the governing flow expressions. These flow expressions are non-dimensioned by employing suitable transformations. The converted flow expressions are computed numerically by applying the MATLAB bvp4c procedure and analytically by the HAM scheme. The impacts of relevant flow factors on fluid velocity, fluid temperature, skin friction coefficient, and local Nusselt number are illustrated via graphs, tables and charts. It is unequivocally shown that the fluid speed declines when escalating the size of the magnetic field parameter; however, it is enhanced by strengthening the Richardson number. The fluid warmness shows a rising pattern when enriching the Biot number and heat consumption/generation parameter. The findings conclusively demonstrate that the surface drag force improves for a larger scale of Richardson number and is suppressed when heightening the unsteady parameter. In addition, it is evident from the outcomes that the heat transfer gradient decreases to increase the quantity of the Eckert number in the convective heating case; however, the opposite nature is obtained in the convective cooling case. Our numerical results are novel, unique and applied in microfluid devices such as micro-instruments, sleeve electrodes, nerve growth electrodes, etc.

Keywords: SWCNTs and MWCNTs; HAM; radiation;joule heating; viscous dissipation; suction/injection

Citation: Prabakaran, R.; Eswaramoorthi, S.; Loganathan, K.; Sarris, I.E. Investigation on Thermally Radiative Mixed Convective Flow of Carbon Nanotubes/Al_2O_3 Nanofluid in Water Past a Stretching Plate with Joule Heating and Viscous Dissipation. *Micromachines* **2022**, *13*, 1424. https://doi.org/10.3390/mi13091424

Academic Editor: Kwang-Yong Kim

Received: 30 July 2022
Accepted: 24 August 2022
Published: 29 August 2022

1. Introduction

The fluid thermal conductivity has been used in many scientific and technical sectors, such as microelectronics, transportation, atomic reactors, heat exchangers, cancer therapy, etc. The ordinary base fluids such as water, oils, ethylene glycol and kerosene have a smaller heat transfer phenomenon because of their weaker thermal conductivity. One of the facile ways to escalate the fluid thermal conductivity is to admix the nanoscale (1–100 nm) particles named nanoparticles into the ordinary base fluids to improve their conductivity. Imtiaz et al. [1] proved that the flow speed is enriched for larger values of the shape parameter and NPVF for the 3D flow of CNTs with the CCHF model. The problem of stagnation point flow of CNTs past a cylinder was analytically solved by Hayat et al. [2]. It has been proved that the NPVF leads to the development of the skin friction coefficient. Yacob et al. [3] noticed that the larger size of NPVF generates more heat inside the boundary for the problem of rotating flow of CNTs on a shrinking/stretching surface. The flow

ISSN: 2395-1680 (ONLINE)
DOI: 10.21917/ijme.2023.0257

OPTIMISING SYSTEM-ON-CHIP ARCHITECTURE USING ASYNCHRONOUS REGRESSION MODEL

P. Kannan[1], P.M. Sithar Selvam[2], T. Priya[3] and S. Murali[4]

[1]*Department of Electronics and Communication Engineering, Francis Xavier Engineering College, India*
[2]*Department of Mathematics, RVS School of Engineering and Technology, India*
[3]*Department of Mathematics, NPR College of Engineering and Technology, India*
[4]*Department of Mathematics, Coimbatore Institute of Technology, India*

Abstract

This paper presents the results of a study that utilises genetic algorithms to optimise the scheduling of tests for a core-based system-on-chip (SoC) system. The research aims at reducing the amount of time that is required to test a SoC system, as well as ensuring that a system meets the requirements of the design. The findings show that it is possible to locate networks that have been carefully tailored to meet the requirements outlined by the RT packets with relation to latency, area, and deadline. The results show that the irregular networks with heterogeneous routers fared much better than the mesh networks when it comes to performance and compliance with the design requirements.

Keywords:

System-On-Chip, Asynchronous Regression Model, Quality of Service, Scalability

1. INTRODUCTION

One capacitor, one transistor, and three resistors were all that were needed to construct the very first integrated circuit ever created. Integrated circuits (ICs) now have architectures known as System-on-Chip (SoC), which comprise billions of transistors. These advancements came about because of breakthroughs in the technology used to fabricate electronic components. The SoC consists of more than a million gates, as well as cores, memory, and both digital and analogue blocks, all of which are packed onto a single chip.

When designing and manufacturing a large-scale integrated circuit, one of the most important challenges that must be surmounted is to find a solution to the issue of temperature control, as well as the problem of power consumption. Because of the high switching activities that are inherent to testing, it is recommended that more time and energy be spent in test mode as opposed to regular mode [1]. This is because testing requires more switching activities than normal mode.

Utilising modular testing of embedded cores is one solution to the testing challenge posed by SoCs. Another solution is to test embedded cores individually. These cores are complex building pieces that have previously been established, which makes design reuse simpler and, therefore, minimises the amount of time that is required for the development of the product. Nevertheless, the production tests and the debugging of those designs are the components of creating SoCs that present the greatest amount of difficulty [2].

The design of the test architecture is required because of this to gain access to the test resources and cores. Thanks to modular testing, SoCs that are outfitted with an Automatic Test Equipment (ATE) Test Access Mechanism (TAM) and embedded cores can communicate with external ATE [3].

Isolating embedded cores is a required step in modular testing, as is getting access to the individual SoCs that will be utilised for the transmission of test data to complete the testing procedure. This method entails the pushing of pre-computed test sets of embedded cores and is performed as part of a divide and conquer strategy.

The modular testing process is driven by these fundamental components [4]. If adequate effort is invested in advance constructing the test infrastructure and organising the tests themselves, it is possible to significantly reduce the cost of the overall testing process. The objective function for this examination is shown by the Eq.(1) that is presented below.

$$T(W_i) = [1 + \max(S_i,S_o)].tp_i + \min(S_i,S_o) \quad (1)$$

The equation is solved by entering the output and input lengths of the scan chain, which are denoted by S_o and S_i, respectively, as well as the test pattern, which is denoted by tp_i. Presentations of benchmark circuits for evaluating SoCs [5].

The scheduling of tests is a fundamental component of system-on-chip (SoC) test automation. A well-thought-out testing strategy will cut expenses and quicken the rate at which the chip will be made available to customers [5]. The proposed approaches offer the additional advantage of lowering test expenses, which is accomplished by cutting down on the amount of time spent on testing, which in turn cuts down on the amount of time spent on testing.

In this article, we discuss regression strategy for scheduling tests with the intention of cutting down on the amount of time as well as the amount of money that is necessary.

2. RELATED WORKS

An Undefined Topology Network on Chip (UTNoC) is described in [6], which may be found here. Each router in this network can interact with any other topology in the system, and each topology can communicate with a single processor. Additionally, each processor can communicate with any other router in the network. Tables are utilised in the process of routing, and the values contained in such tables are distributed to various locations. Every router in the UTNoC network can communicate with every other router in the topology. Every router in the network can have a sizable number of ports.

Experiments were performed on the UTNoC network utilising a simulator constructed with SystemC. to optimise the network and get results that are comparable to those of the application graph, the tool makes use of a genetic algorithm to cut ties between the routers. This allows the tool to accomplish the desired outcomes. Because of this, the technology can generate findings that are more precise [7].

IJCRT.ORG ISSN : 2320-2882

INTERNATIONAL JOURNAL OF CREATIVE RESEARCH THOUGHTS (IJCRT)

An International Open Access, Peer-reviewed, Refereed Journal

Bipolar Quadripartitioned Neutrosophic Soft Set

[1]M. Ramya, [2]S. Murali, [3]R.Radha

[1]Assistant Professor, Jansons Institute of Technology,Karumathampatti.
[2]Assistant Professor, Department of Mathematics, Coimbatore Institute of Technology, Coimbatore.
[3]R.Radha, Research Scholar, Department of Mathematics, Nirmala College for Women, Coimbatore

Abstract: The aim of this paper is to introduce the concept of bipolar quadripartitioned neutrosophic soft set and its properties are studied.

Keywords – neutrosophic set, neutrosophic soft set, quadripartitioned neutrosophic set, quadripartitioned neutrosophic soft set, bipolar neutrosophic set, bipolar quadripartitioned neutrosophic soft set.

I. INTRODUCTION

The fuzzy set was introduced by Zadeh [23] in 1965. F. Smarandache introduced the idea of the Neutrosophic set. It is a mathematical method for handling issues involving unreliable, indeterminate and inconsistent details.

A neutrosophic set[20] is proposed by F. Smarandache. The indeterminacy membership function walks along independently of the membership of the truth or the membership of falsity in neutrosophic sets. Neutrosophic theory has been extensively discussed in the treatment of real life conditions involving uncertainty by researchers for application purposes.

While the hesitation margin of neutrosophical theory is independent of membership in truth or falsehood, it still seems more general than intuitionist fuzzy sets. Recently, the relationships between inconsistent intuitionistic fuzzy sets, image fuzzy sets, neutrosophic sets, and intuitionistic fuzzy sets have been examined in Atanassov et al.[3]; however, it remains doubtful whether the indeterminacy associated with a particular element exists due to the element's ownership or non-belongingness. Chatterjee et al.[4] have pointed out this while implementing a more general structure of neutrosophic set viz. quadri partitioned single valued neutrosophic set (QSVNS). Molodtsov [8] first proposed the idea of Soft Sets as an entirely new mathematical method to solve problems dealing with uncertainties. A soft set is defined by Molodtsov [8] as a parameterized family of universe set subsets where each member is regarded as a set of approximate elements of the soft set. In the past few years, different researchers have researched the foundations of soft set theory.

Ramesh Kumar [16] initiated the idea of quadripartitioned neutrosophic soft sets and its topological spaces. Also he introduced the concept of pentapartitioned neutrosophic soft sets. Mumtaz Ali [9] introduced the concepts of bipolar neutrosophic soft sets and its application in decision making. The bipolar neutrosophic set was proposed by Ali et al.

This paper is dedicated to propose bipolar quadripartitioned neutrosophic soft set which is a hybrid structure of soft set and bipolar quadripartitioned neutrosophic set. Firstly, we introduce the bipolar quadripartitioned neutrosophic soft set and discuss some basic properties with illustrative examples

II. PRELIMINARIES

2.1 Definition [20]

Let X be a universe. A Neutrosophic set A on X can be defined as follows:

$$A = \{< x, T_A(x), I_A(x), F_A(x) >: x \in X\}$$

Where $T_A, I_A, F_A: U \to [0,1]$ *and* $0 \leq T_A(x) + I_A(x) + F_A(x) \leq 3$

Here $T_A(x)$ is the degree of membership, $I_A(x)$ is the degree of inderminancy and $F_A(x)$ is the degree of non-membership.

2.2 Definition [7]

Let X be a universe. A Quadripartitioned neutrosophic set A with independent neutrosophic components on X is an object of the form

$$A = \{< x, T_A(x), C_A(x), U_A(x), F_A(x) >: x \in X\}$$
$$and\ 0 \leq T_A(x) + C_A(x) + U_A(x) + F_A(x) \leq 4$$

Here $T_A(x)$ is the truth membership, $C_A(x)$ is contradiction membership,$U_A(x)$ is ignorance membership and $F_A(x)$ is the false membership.

Discrete Mathematics, Algorithms and Applications | Vol. 15, No. 05, 2250128 (2023)

Research Paper

More on the outer connected geodetic number of a graph

K. Ganesamoorthy and D. Jayanthi

https://doi.org/10.1142/S1793830922501282 | Cited by: 1

< Previous Next >

Abstract

For a connected graph $G = (V, E)$ of order at least two, a *total outer connected geodetic set* S of a graph G is an outer connected geodetic set such that the subgraph induced by S has no isolated vertices. The minimum cardinality of a total outer

https://doi.org/10.37896/sr10.5/012

Prediction of Technical Efficiency in Farming

Mary Louis L and Sangeethamani S***

**Professor, Kumaraguru College of Liberal Arts and Science*

***Assistant Professor, Coimbatore Institute of Technology*

Abstract

In the present farming scenario, efficiency is the greatest concern of researchers with an aim to investigate the determinants of efficiency levels of farmers. One of the components of efficiency viz., Technical Efficiency (TE) can be measured using the Stochastic Frontier Model as it considers Stochastic noise into account. The present study measured the Technical Efficiency Score (TES) of 180 sample turmeric farms using the Translog Normal Truncated Normal Stochastic Frontier Model (TNTNSFM). The result using TNTNSFM showed that the input manure played a major role in better turmeric production. According to this model, more than 41 percent of the difference between the observed output and frontier output was primarily due to factors, which were under the control of farmers. The minimum technical efficiency estimated using TNTNSFM was 80.93 percent while the maximum was 90.42 percent. The mean level of technical efficiency was 85.23 percent which showed that only 85.23 percent of technical abilities were realized by sample farmers. Hence, on average 14.77 percent of the technical potentials were not realized in the case of raising turmeric crops in the northwestern region of Tamil Nadu. Moreover, the highest number of farms (99) were found in the efficiency class of 85-90 percent followed by 80-85 percent (80). Only one farm lies in the efficiency score of 90-95 percent. The correlation coefficient between observed efficiency and technical efficiency using TNTNSFM was given by $r_{OE} = 0.544$ which was found to be the least among translog stochastic frontier models. The Chi-square value of TNTNSFM was obtained as 6.3689.

Key Words: Technical efficiency, Stochastic Frontier model, Maximum Likelihood Estimate, Production Function.

Introduction

The possibility of India being a substantial exporter of agricultural commodities is very high if India globalizes its agriculture. However, if this dynamic future for Indian agriculture is to be achieved, a number of critical requirements must be met. The first and most important is to secure and sustain high production growth rates. This calls for continuous improvement in productivity. The agricultural productivity of a production unit, defined as the ratio of its output to its input, varies due to differences in production technology and differences in the efficiency of the production process (Mythili, G and K.R. Shanmugam,2000). The efficiency of a production unit may be defined as how effectively it uses variable resources for the purpose of profit maximization, given the best production technology available. The concept of efficiency is further divided into two components technical efficiency and allocative efficiency. Traditionally, researchers have concentrated on the study of allocative efficiency based on the assumption that entrepreneurs operate on technical production functions with full technical efficiency (Kalirajan, K.P., 1999). However, in recent literature, it is seen that the above assumption is weak and several farmers do not realize the full potential of technology due to several factors such as their managerial skills and differences in the production environment (Seung *et al.*,2007).

Journal of Positive School Psychology
2022, Vol. 6, No. 4, 7220 – 7225

http://journalppw.com

Traits of Nano regular weakly neighbourhood and Nano regular weakly closed map in Nano Topological space

[1]S. Dayana Mary, [2]C. Indirani, [3]K. Meenambika

[1]*Department of Mathematics, Coimbatore Institute of Technology, sdayanamary@cit.edu.in*
[2]*Department of Mathematics, Bannari Amman Institute of Technology, indiranic@bitsathy.ac.in*
[3]*Department of Mathematics, Sri Shanmuga College of Engineering &Technology, Sathyamangalam, Erode, India Sankari, India, meenabalaji08@gmail.com*

Abstract

The aim of this paper is to introduce new forms of neighbourhood called Nano regular weakly neighbourhood. In addition, we define Nano regular weakly closed maps also various properties and characterizations related to these functions are also examined and investigate some of their properties.

Keywords: Nrw-neighbourhood and Nrw-closed map.

I. INTRODUCTION

In the past few decades, there has been a significant increase in the applications of Topology in fields as diverse as Medicine, Engineering, Economics, Chemistry, Computer Science, Cosmology. Topology has gained access to human interventions to make life easier. In recent years, mathematicians use topology to model and give solutions to the real world problems. Many different versions of generalized closed maps and related topological properties were introduced by eminent Mathematicians.

Stone [1] and Tong [2] defined and investigated Regular open sets and strong regular open sets respectively. Cameron [3] introduced and analyzed the weaker form of regular open sets called a regular semiopen set. Benchalli et. al., [4] defined and studied RW-closed sets.

Many different versions of generalized closed maps and related topological properties were introduced by eminent Mathematicians. Long and Herrington [5] studied the properties of regular closed functions. Malghan [6] were introduced and studied Generalized closed mappings. The notion of generalized pre-closed functions and semi regular weakly closed maps were introduced and studied by Noiri et., al., [7] and Wali et. al., [8] respectively.

Palwak [9] defined and discussed the notion of rough sets. The idea of nano topological space was initiated by Lelli's Thivagar [10] in terms of lower, upper approximations and its boundary regions. He applied set valued ordered information system for attribute reduction in nutrition modelling. The nano α-open sets, nano semi-open sets, nano pre-open sets and nano regular-open sets are also studied in [10]. Dayana Mary S et.al. [11] introduced and analyzed nano regular weakly closed set in nano topological spaces.

P. Sathishmohan et.al [12] introduced and investigated the properties of nano semi pre-neighbourhoods. K. Chitrakala et., al., [13] defined and discussed Some generalization of neighbourhoods in nano topological spaces.

Lelli's Thivagar [14] introduced and studied a Nano closed map in Nano Topological Space. M. Bhuvaneswari and N. Nagaveni [15] defined and investigated Nwg-closed map in Nano

JOURNAL OF ALGEBRAIC STATISTICS
Volume 13, No. 3, 2022, p. 1657-1664
https://publishoa.com
ISSN: 1309-3452

INTUITIONISTIC FUZZY IN NANO TOPOLOGICAL SPACES

[1]C. Indirani, [2] S. Dayana Mary, [3]K. Meenambika

[1]Department of Mathematics, Bannari Amman Institute Of Technology - Sathyamangalam

[2]Department of Mathematics, Coimbatore Institute of Technology-Coimbatore .

[3]Department of Mathematics, Sri Shanmuga College of Engineering and Technology-Sankari. .

Email id: indiranic@bitsathy.ac.in, sdayanamary@cit.edu.in, meenabalaji08@gmail.com

Abstract: *The scope of this paper is to give introduction and basic on intuitionistic fuzzy nano topology, intuitionistic fuzzy nano topological spaces, Basic properties of intuitionistic fuzzy nano open sets and intuitionistic fuzzy nano closed sets are studied.*

Keywords and Phrases: *Lower approximation, Upper approximation, Boundary region, Equivalence relation, Intuitionistic fuzzy set, Intuitionistic fuzzy topology and Intuitionistic fuzzy Nano-open sets, Intuitionistic fuzzy Nano-closed sets, Intuitionistic fuzzy Nano-closure and Intuitionistic fuzzy Nano interior in topological spaces.*

2000 AMS Classification. 03F55 , 54A40 , 54A10 , 54A20.

1.Introduction

The concept of nano topology was first introduced by Lellis Thivagar[5] in which the terms of approximations and boundary region and equivalence relation of a subset are discussed and defined the nano closed sets, nano interior and nano-closure in topological space. Fuzzy set was proposed by Zadeh[10] in 1965, it shows a degree of membership for each member of the set to a subset of it. The

Journal of Intelligent & Fuzzy Systems 44 (2023) 4323–4334
DOI:10.3233/JIFS-221430
IOS Press

Optimized scheduling with prioritization to enhance network sustainability in edge-cloud environment

K.N. Apinaya Prethi[a,*], M. Sangeetha[b] and S. Nithya[a]
[a]*Assistant Professor, Kumaraguru College of Technology, Coimbatore*
[b]*Department of Information Technology, Coimbatore Institute of Technology, Coimbatore*

Abstract. Due to decentralized infrastructure in modern Internet-of-Things (IoT), the tasks should be shared around the edge devices via network resources and traffic prioritizations, which weaken the information interoperability. To solve this issue, a Minimized upgrading batch Virtual Machine (VM) Scheduling and Bandwidth Planning (MSBP) was adopted to reduce the amount of batches needed to complete the system-scale upgrade and allocate the bandwidth for VM migration matrices. But, the suboptimal use of VM and possible loss of tasks may provide inadequate Resource Allocation (RA). Hence, this article proposes an MSBP with the Priority-based Task Scheduling (MSBP-PTS) algorithm to allocate the tasks in a prioritized way and maximize the profit by deciding which request must handle by the edge itself or send to the cloud server. At first, every incoming request in its nearest fog server is allocated and processed by the priority scheduling unit. Few requests are reallocated to other fog servers when there is an inadequate resource accessible for providing the request within its time limit. Then, the request is sent to the cloud if the fog node doesn't have adequate resources, which reduces the response time. However, the MSBP is the heuristics solution which is complex and does not ensure the global best solutions. Therefore, the MSBP-PTS is improved by adopting an Optimization of RA (MSBP-PTS-ORA) algorithm, which utilizes the Krill Herd (KH) optimization instead of heuristic solutions for RA. The simulation outcomes also demonstrate that the MSBP-PTS-ORA achieve a sustainable network more effectively than other traditional algorithms.

Keywords: Internet-of-things, edge devices, resource allocation, priority levels, task scheduling, krill herd optimization

1. Introduction

Internet-of-Things (IoT) is rapidly evolving with the requirement to link real-time with the web [1, 2]. These systems typically include sensor and edge node layers. More sensors in a sensor layer are expected to exceed 50 billion in the upcoming centuries with a large majority of sensors having specific functionalities and so data interoperability is challenging [3]. In terms of scalability, energy conservation, knowledge, transmission, integration, dependability, semantics, output and standards, the IoT challenges are extremely flexible [4]. The recent methods and concepts must simply be integrated for network resources, in particular in harsh mobile scenarios like vehicle communications and in smart environments such as cities, homes and industries that support seamless connectivity between different accessing technologies [5]. The growth of IoT systems and services cannot achieve a global level in several industrial sectors without globally recognized and interoperable standards. A single middleware sensor is frequently needed to handle a huge amount of information from various data sources [6, 7]. Recent IoT specifications provide middleware solutions for identifying specific global identity criteria such as

*Corresponding author. K.N. Apinaya Prethi, Assistant Professor, Kumaraguru College of Technology, Coimbatore. E-mail: abipreethu@gmail.com.

ISSN 1064-1246/$35.00

data fusion, scalability and interoperability to serve all-IP-based transmissions [8, 9].

Since IoT technologies are complex and diverse, a single interoperability solution can be inadequate and integration is essential. To resolve the new challenges, interoperability of IoT technologies will always be a complex theme [10]. This can be done by enhanced embedded intelligence and virtualization with cognitive abilities. But, several problems can be overcome such as cost, scalability, resource use and how resources can be distributed more efficiently with network sustainability [11]. Virtualization offers a cost-effective solution to this challenge. The data obtained by multiple sensors is virtualized and transmitted into the VM by the same system. Each edge device on the edge device layer copes with neighboring VMs in which computing abilities for sensor information from the sensing region are encapsulated for alleviating an additional price and latency for migrating VMs to the remote cloud [12]. Additionally, edge devices can also schedule local VMs dynamically by consulting with other edge devices.

Various resource distribution techniques were suggested in earlier days to address the VM planning for improving the sustainability and performance of the network's edge devices [13]. To recycle the edge devices in IoT networks, a sustainable strategy [14] was suggested. At first, the minimum upgrading batch VM allocation challenge was described such as NP-hard evidence, probability state suggestion and minor limit testing. Then, the MSBP was designed. Initially, a greedy strategy was applied to reduce the amount of batches needed to complete the network-level upgrading. Then, the VM migration matrix per batch was obtained. Also, two strategies such as Shortest Trajectory First (STF) and Least Bandwidth Utilization First (LBUF) were applied to allocate the trajectories and bandwidth for VM migration matrices. In STF, the minimum space relocation path was found along the optimal links which contain high accessible remaining bandwidth. Also, the transmit energy was determined for the edge devices for forwarding the sensed information. However, the suboptimal use of VM and possible loss of tasks may provide inadequate resource distribution.

Hence in this research article, an MSBP-PTS algorithm is proposed with MSBP to assign the tasks in a prioritized manner and achieve the maximum profit. The main aim of this MSBP-PTS is to decide which request should handle by the edge itself or forward to the cloud server. This algorithm consists of two phases depending on the network structure where a fog layer is employed between the end-users and the cloud server. Initially, each inward request in its closest fog server is assigned and each request within the fog server is placed in a suitable priority queue followed by the priority scheduling unit. Then, every request in the priority queues within a fog server is processed and few requests are reassigned to other fog servers while there is inadequate resource accessible for serving the request within its time limit. At last, the incoming task is transmitted to the server at center while the edge layer doesn't contain adequate resources for providing the request. Based on this algorithm, the response time is reduced when the considerable cost is also decreased. A larger throughput decreases the average response period and the overall price because of its ability to efficiently prioritize jobs based on their latency acceptance ranges. But, the MSBP is the heuristics solution that does not ensure the global optimal solutions efficiently and is also very expensive. As a result, the MSBP-PTS-ORA algorithm is proposed in which the KH optimization algorithm is applied instead of using heuristic solutions to optimize the resource allocation effectively. In this algorithm, the NP-hard problem is solved by using the KH algorithm. Each member of the KH will make their contribution to the transition activity, based on their fitness. It is based on krill behavior. Because of the krill's total fitness, it is possible to pick the appropriate global assessment of its food center. Foraging behavior and randomized diffusion are used to calculate a krill's position over time. Based on the best global solution, the NP-hard problem is solved that minimizes the batch size when maintaining the provision stability via VM migration. As a result, the major contributions of this study are:

- First, the MSBP-PTS algorithm is proposed with MSBP to determine which task request must handle by the edge itself or transmit to the cloud server. In this algorithm, the tasks are allocated in a prioritized manner and the maximum profit is achieved.
- Additionally, the ORA algorithm is introduced based on the KH optimization scheme rather than applying heuristic solutions for assigning the optimal resources during VM migration. Thus, optimality of MSBP is ensured and the network sustainability is effectively improved by this algorithm.
- Further, the extensive outcomes illustrate that the MSBP-PTS-ORA accomplishes a better

efficiency during VM migration compared to the MSBP and other standard algorithms.

Following are the arrangements for the remaining manuscript: The relevant works are discussed in Section 2. The presented algorithm is stated in Chapter 3, and its simulation results are shown in Section 4. The complete study is covered in Section 5 along with suggestions for improvement.

2. Literature survey

For mobile edge computing, a dynamic resource and computational offloading paradigm [15] with privacy protection were suggested. For multiuser settings, the computing and radio resources were first evaluated together to ensure effective resource sharing. In addition, the AES encryption method was used to safeguard confidential information from hackers. A unified framework has been created to reduce the overall system's time and energy usage. Finally, a compute offloading technique with comprehensive procedures was created for mobile subscribers.

A new bio-inspired hybrid algorithm (NBIHA) was created by Hina et al. (2019) by fusing customized particle swarm optimization and cat swarm optimization (MCSO). Particle swarm optimization was applied to allocation of resources, and cat swarm optimization was applied to managing resources [16]. Zubair et al. (2021), edge computing defines dynamic and priority-dependent resource allocation. The A-PBRA dynamic resource allocation system presented enables efficient resource utilisation within the EC paradigm. After an incoming request has been classified as either usual or prioritised, there are three possible outcomes. The accessible resources are therefore distributed in line with the priority of the user requests in order to stay within the limits [17].

The MORA [18] polynomial time technique enables the network administrator to maximise its profitability, which can be enhanced user Quality-of-Experience (QoE), inter-domain congestion reductions, or other pertinent metrics. As a result of this technique, services may adapt to the network operator's resources and rely on the cloud for additional computing. Micro-service architecture, which breaks down a particular service into a series of pieces that MORA places in multiple computing nodes of the edge, was also well-suited, and multi-dimensional resources were efficiently managed.

For the data-driven, deep reinforcement learning-based scheduling for edge-cloud situations, an architectural network paradigm [19] was designed. For scheduling in distributed deployments, a general asynchronous training technique was intended. Then, a chaotic dynamic scheduling strategy using policy gradient-based reinforcement learning is presented. A fog-enabled structure [20] was presented to handle the task scheduling requests and achieve the best outcomes. Then, the task scheduling issue was formulated as an Integer Linear Programming (ILP) optimization scheme according to the time and fog power usage. This was resolved by the Opposition-based Chaotic Whale Optimization Algorithm (OppoCWOA) on time.

For fog-cloud resources in a nonprofit computing system, a joint Quality-of-Service (QoS)-aware and cost-effective job scheduling method [21] has been developed. This algorithm's primary objective was to reduce the cost of computation, communication, and delay violations for Internet of Things requests. In a cloud services, a meta-heuristic model called MDVMA [22] has been introduced for dynamic VM assignment with optimum work scheduling. The Non-dominated Sorting Genetic Technique (NSGA)-II algorithm was used to optimise job scheduling while lowering power consumption, makepan, and cost concurrently to achieve trade-offs with the providers of cloud services in accordance with their requests.

The Cloud-based Object Tracking and Behavior Identification System (COTBIS) [23] has been developed, which includes the edge computing ability at the gateway level. Initially, each unnecessary frame in the edge level was filtered and the significant frames were sent to the cloud to minimize the bandwidth needed for data transfer. Then, robust object identification and fall recognition schemes were conducted in the cloud data center based on the background subtraction and deep learning models, which reduce the response period.

In the cloud-fog paradigm, a semi-adaptive real-time task scheduling technique [24] has been introduced to express job scheduling as a possible combination optimization method. To find various combinations for incoming tasks at all scheduling cycles, a customized genetic algorithm was used. Following that, the jobs were assigned to the VM based on the best permutation. A hungarian algorithm-based pair-based job scheduling method [25] for the cloud computing environment. An uneven number of tasks and workloads were taken into account in this

Table 1
Summary of various algorithms for task and resource allocation in edge-cloud environment

Ref. No.	Algorithm	Achievements	Limitations
[15]	Dynamic resource and computational offloading paradigm with AES encryption	It chooses a few computation tasks to offload when neglecting others optimally so that the total overhead of the network was reduced.	While offloading computing tasks in low-bandwidth mode, the amount of information was large.
[16]	NBIHA	It obtains better scheduling efficiency.	The computational complexity was considerable and an optimal distribution of resources was not thought about.
[17]	A-PBRA	Ability to manage a greater volume of incoming jobs while also maximising the use of the edge node's limited resources.	Requests can be furthermore prioritized.
[18]	MORA	It highly improves the utility.	It requires further improvement by considering the appropriate resources and utility forecasting
[19]	A policy gradient-based deep reinforcement learning-based scheduling	It was a preferable option for dynamic scheduling tasks in unpredictable circumstances since it has a small scheduling overhead.	It needs fixed resources for new tasks in real-time scenarios.
[20]	OppoCWOA-based task scheduling	It achieves time-energy-efficient task scheduling.	It did not consider the scenario, where task execution was unsuccessful on the fog node because of the CPU destruction. Also, it did not consider the task migration between fog/cloud nodes.
[21]	Joint QoS-aware and cost-efficient task scheduling algorithm	It enhances the deadline satisfaction task rates and reduces the overall cost of task scheduling.	When increasing the number of volunteer computing systems, the power usage by their computing resources also increased, which results in a considerable effect on the system cost.
[22]	MDVMA	It was a workable and beneficial way to achieve optimal task scheduling while consuming less time, energy, and money.	It did not consider the response time and network latency, which also need to increase the efficiency of task scheduling.
[23]	COTBIS	It minimizes the network bandwidth and response time.	It cannot balance the real-time tasks among edge devices.
[24]	Semi-adaptive real-time task scheduling scheme	It improves the trade-off between the overall execution cost and the ease of implementation and lowers the job failure rate.	It has a high elapsed run time while increasing the number of tasks. Also, the resources of the VM situated in the fog node were assumed to be restricted compared to the VMs situated in the cloud nodes.
[25]	Pair-based task scheduling algorithm	It can be used to decrease idle time and arrange the jobs efficiently.	It did not validate using a large number of tasks and clouds. Also, the dynamism of CPU and network usage was not considered. The network delay between the clients/tasks was not flexible.

algorithm, along with task matching to generate the scheduling solution.

Table 1 summarizes the above-studied algorithms in the edge-cloud paradigm for task scheduling and RA according to their achievements and limitations.

2.1. Research gap

From literature, it is observed that various kinds of task scheduling and RA algorithms have been suggested for edge-cloud computing paradigm. But, each algorithm has its specific limitations, which needs to solve by developing advanced algorithms. Also, the resource sharing was not satisfactory for suboptimal utilization of VM and possible loss of tasks. So, this article focuses on solving these problems by considering the priorities of the tasks and optimal resources during VM migration.

3. Proposed methodology

In this section, the MSBP-PTS and MSBP-PTS-ORA algorithms are explained in detail. Mainly, virtualized server is the major unit of resource distribution that increases the total response period and the rate of network utilization.

3.1. MSBP with priority-based task scheduling

3.1.1. Design model

This takes into consideration a cloud-fog environment that consists of cloud, fog, and consumer layers.

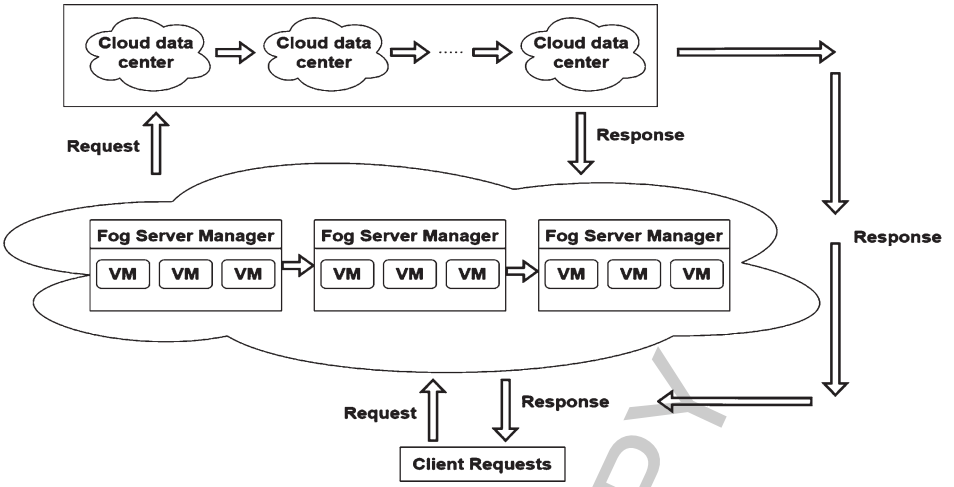

Fig. 1. Structure of resource distribution in fog and cloud layer.

The procedure is carried out on the fog layer, which initially checks whether the associated energy in fog nodes can meet customer needs. The demand is sent to the central cloud if there are no available resources that are sufficient. The fog node algorithm then performs each customer's requests and executes them in accordance with their priority levels.

Figure 1 illustrates the considered fog-cloud structure, which describes the following:

- The upper level is the cloud level, which encompasses the cloud data centers.
- The mid-level is the fog level, which comprises more fog nodes, or fog servers with micro data centers and VMs. In all fog servers, the resources such as processors and VMs are controlled by the fog server manager.
- The lower level is the user level, in which all users transmit requests to their adjacent fog server.
- By accepting the user request, the fog server manager implements the below processes:
  1. The request is dismissed if it cannot be completed before the deadline.
  2. Or else, the fog server manager chooses the priority queue for the request based on its priority, timeframe and accessible resources.
- The requests in the priority queues are handled by the fog server manager in the prioritization order. For all requests:
  1. When each resource needed by the request is accessible on the allocated fog server, the request is processed and the outcome is transmitted to the user.
  2. When the resources needed are fulfilled by the edge layer, the request (which is divided into sub-tasks) is transmitted to single or multiple residual fog servers in the fog layer.
  3. The request is sent to the central cloud for execution if there are no suitable resources available in the fog layer.

3.1.2. *Queuing and priority model*

User requests may have several deadlines that need to be met for the work to be finished on time. Accordingly, the fog layer implements the priority scheduling method. Assumptions of this algorithm are the following:

- There are three priority levels (queues): high, average and low.
- The provision period of all requests from the customer i i.e., (req_i) is computed as:

$$delay_i^T = DL_i^T - C_i^T \tag{1}$$

In Eq. (1), $delay_i^T$ is the extreme tolerable time of req_i, C_i^T is the current time and DL_i^T is the time limit provided by req_i.

The estimated overall provision period $\left(ST_{est}^T\right)$ needed by each job in the 3 priority queues is

computed as:

$$ST_{est}^{T} = \sum_{i=1}^{Y} ST_{est,i} \tag{2}$$

Where

$$Y = |Q_H| + |Q_M| + |Q_L| \tag{3}$$

Here, $ST_{est,i}$ indicates the estimated provision period needed by req_i, Q_H, Q_M and Q_L are high, medium and low priority queues, respectively. In accordance with the request's latency and priority type, it is placed in any queue. The overall period req_i used in the fog layer is given by,

$$W_i = W_i^{Q} + \mu_i \tag{4}$$

In Eq. (4), W_i^{Q} refers to req_i used in the queue and μ_i refers to the overall provision period consumed by req_i. The greatest latency $\left(delay_i^{T}\right)$, a request is permitted in the specific SLA. To achieve this QoS necessity for req_i,

$$W_i < delay_i^{T} \tag{5}$$

3.1.3. Priority assignment module

This module has two main phases. The first phase allocates each incoming request to its nearby fog server and locates the request in a proper priority queue within the fog server. In this phase, once the incoming request is allocated to the nearby fog server, its greatest accepted latency is computed by Eq. (1).

After that, it verifies if all the resources i.e., the total amount of processors accessible at the fog layer could achieve the greatest accepted latency. Or else, the request is discarded directly. Else, the request is located in one of the priority queues.

The second phase executes the requests in the fog server through the priority queues depending on their priority. Then, the request is provided at the present fog server, if the fog server contains the adequate resource to fulfill the request's delay time and reach its time limit using Eq. (5). Otherwise, the request is reallocated to the other fog server via implementing the first phase on the fresh fog server; when the demanded job is huge and requires a high amount of resources, the job is split into sub-jobs and allocated to various fog servers. At last, if there is inadequate resource accessible in the whole fog layer, then the demand is transmitted to the central server.

Pseudocode for Prioritized Task Scheduling

Step 1: Allocate all requests in the fog server and in a priority queue
For all requests do
Each request is broadcasted to the nearby fog server;
Calculate delay for each request using Eq. (1);
if $\left(\left(\frac{ST_{est}^{T}}{C} + ST_{est,i}\right) > delay_i^{T}\right)$*/*Verify deadline*/ //C: number of fog servers*
The request is rejected;
else if */*Initial effort for providing in fog layer*/*
*/*Locate in a priority queue by the priority scheduling unit */*
$(Pr_i) = Priority\left(delay_i^{T}, ST_{est}^{T}\right)$;
if $(Pr_i == High)$
Locate request in Q_H;
else if $(Pr_i == Medium)$
Locate request in Q_M;
else if $(Pr_i == Low)$
Locate request in Q_L;
Step 2: Process request in fog server or in cloud
*For all high, medium and low requests do /*Requests served based on priority levels*
while $(Q_x \neq \emptyset)$
For all requests in Q_x *do*
if $(adequateresourcesincurrentfogserver)$ */*Eq. (5) remains*/*
Provide the request in the present fog server;
else if $(adequateresourcesinfoglayer)$
Assign resources from the remaining fog server, following Step 1, split tasks into sub-jobs if required;
else */*no adequate resource in fog group*/*
Transmit the request to the cloud;

Thus, the total response time is reduced when decreasing the considerable rate. Since this algorithm can prioritize the jobs based on their latency acceptance and priority levels resulting in greater efficiency and lesser mean response time. As the MSBP is the heuristic solution; it requires knowledge and experience to apply the heuristics effectively and it does not guarantee the global optimal solutions. As a result, optimized resource allocation is proposed by using the KH optimization algorithm.

3.2. MSBP-PTS with optimized resource allocation using KH optimization

In PLAOR, In this algorithm, the NP-hard problem i.e., least batch VM scheduling is solved by optimizing the VMs resource demand which enables the KH often reach the best rate, hence providing the least

amount of batches. As with krill, each KH member contributes to the movement process based on their fitness. Because of the krill's total fitness, it is possible to identify the best global assessment of its food center. Foraging behavior and random dispersion are used to calculate the krill's time-dependent position. The KH approach searches the solution space using a d-dimensional Lagrangian notion.

$$\frac{dD_i}{dt} = MI_i + FA_i + RF_i \tag{6}$$

In Eq. (6), MI_i is the krill's motion stimulation, FA_i is the foraging motion and RF_i is the random diffusion. Various parameters are initialized such as highest iteration (max_{Itn}), greatest stimulated velocity (max_{IS}), greatest diffusion velocity (max_{DS}), maximum foraging speed (max_{FS}), amount of krill (Nbr), location of krill (D) and amount of resources (Nbr_R). The amount of resources considered is equivalent to the amount of krill. Once the process is initiated, it creates the location of resources randomly. For each location of current resources, the fitness of each krill is determined.

1) *Krill Individual Movement Induction:* The motion is caused by the krill's effort to retain a greater population. The movement owing to other krill individuals is determined as:

$$MI_i^{new} = max_{IS}\delta_i + w_{nbr}MI_i^{old} \tag{7}$$

In Eq. (7), $w_{nbr} \in [0, 1]$ is the inertia weight with the movement stimulated and MI_i^{old} is the last motion induced.

$$\delta_i = \delta_i^{local} + \delta_i^{target} \tag{8}$$

Here, δ_i^{local} is the neighbor's local effect and computed as:

$$\delta_i^{local} = \sum_{j=1}^{Nbr_n} \hat{K}_{i,j}\hat{D}_{i,j} \tag{9}$$

Where

$$\hat{D}_{i,j} = \frac{D_j - D_i}{||D_j - D_i|| + t} \tag{10}$$

$$\hat{K}_{i,j} = \frac{K_i - K_j}{K_{worst} - K_{best}} \tag{11}$$

In Eq. (11), K_{best} and K_{worst} are the most excellent and the most unpleasant krill rates, accordingly, K_i is the fitness of i^{th} krill, K_j is the fitness of j^{th} neighbor, t is a diminutive optimistic integer and Nbr_n is the number of neighbors. The sensing distance for each krill is computed as:

$$dist_{s,i} = \frac{1}{5 \times Nbr}\sum_{j=1}^{Nbr} \|D_i - D_j\| \tag{12}$$

In Eq. (12), D_i and D_j are the related location of i^{th} and j^{th} krill. When the space between D_i and D_j is smaller than the definite observing space, D_j is an adjacent of D_i. The effect of target direction δ_i^{target} is obtained using the most excellent krill as:

$$\delta_i^{target} = A_{best}\hat{K}_{i,best}\hat{D}_{i,best} \tag{13}$$

In Eq. (13), A_{best} is the krill's valuable coefficient with the most excellent fitness to i^{th} krill and determined as:

$$A_{best} = 2\left(r + \frac{I_a}{max_{Itn}}\right) \tag{14}$$

In Eq. (14), $r \in [0, 1]$ is the random value and I_a denotes the actual iteration number.

2) *Mobility because of Foraging Motion:* It is represented depending on the food position and prior knowledge regarding the food position as follows:

$$FA_i = max_{FS}\varepsilon_i + w_{FS}FA_i^{old} \tag{15}$$

In Eq. (15), $w_{FS} \in [0, 1]$ is the inertia weight of foraging activity and ε_i^{best} is i^{th} krill's most excellent fitness until now.

$$\varepsilon_i = \varepsilon_i^{food} + \varepsilon_i^{best} \tag{16}$$

The food attractiveness ε_i^{food} is determined as:

$$\varepsilon_i^{food} = A^{food}\hat{K}_{i,food}\hat{D}_{i,food} \tag{17}$$

In Eq. (17), A^{food} is the food coefficient and determined by

$$A^{food} = 2\left(1 - \frac{I_a}{max_{Itn}}\right) \tag{18}$$

The effect of the best fitness of i^{th} krill is determined as:

$$\varepsilon_i^{best} = \hat{K}_{i,ibest}\hat{D}_{i,ibest} \tag{19}$$

In Eq. (19), $\hat{K}_{i,ibest}$ and $\hat{D}_{i,ibest}$ is i^{th} krill's earlier stayed most excellent fitness and location, accordingly. Then, the food center is computed for each

iteration as:

$$D^{food} = \frac{\sum_{i=1}^{Nbr} \frac{1}{K_i} D_i}{\sum_{i=1}^{Nbr} \frac{1}{K_i}} \tag{20}$$

3) *Physical Dispersion:* It is represented regarding dispersion velocity and an arbitrary directional vector as:

$$RF_i = max_{DS} \left(1 - \frac{I_a}{max_{Itn}}\right) \beta \tag{21}$$

Where $\beta \in [-1, 1]$ is the random directional vector.

4) *Updating Position:* The location of krill is updated for a different amount of resources. Further, the efficiency of the KH algorithm is improved by combining the crossover and mutation processes.

3.2.1. Crossover

Consider $d_{i,s}$ be the s^{th} component of D_i and determined by the following equation:

$$d_{i,s} = \begin{cases} d_{t,m}, \ r_{i,m} < C_0 \\ d_{i,m}, \quad else \end{cases} \tag{22}$$

In Eq. (22), C_0 is the crossover probability which is equal to $0.2\hat{K}_{i,ibest}$.

3.2.2. Mutation

$$d_{i,m} = \begin{cases} D_{gbest,m} + > \rho \left(d_{p,m} - d_{q,m}\right), \ r_{i,m} < M \\ d_{i,m}, \qquad\qquad Or\ else \end{cases} \tag{23}$$

In Eq. (23), M is the mutation probability which is equal to $\frac{0.05}{\hat{K}_{i,ibest}}$. A krill's location vector during a period $[tm, tm + \Delta tm]$ is computed based on various parameters of the movement as:

$$D_i\,(tm + \Delta tm) = D_i\,(tm) + \Delta tm \frac{dD_i}{dt} \tag{24}$$

The optimal resources linked to the overall best krill are chosen after the process has proceeded through the maximum number of iterations. In order to effectively solve NP-hard server aggregation or VM migration challenges, the resource allocation of the fog servers (edge devices) is optimized.

Pseudocode for KH-based Optimized Resource Allocation

Input: Number of resources, fog servers and VMs;
Output: Most optimal resources
Initialize $max_{Itn}, max_{IS}, max_{DS}, max_{FS}, Nbr, D$ and Nbr_R;
Generate the location of resources randomly;
Compute the fitness of the current resource according to its location;
while $(I_a > max_{Itn})$
Order the krill inhabitants from the most excellent to most unpleasant;
For every krill individual do
Compute the motion induced by other krills using Eqns. (7)–(14);
Compute foraging motion using Eqns. (15)–(20);
Evaluate the physical diffusion motion using Eqns. (21);
Apply crossover probability and mutation probability;
Update location for each krill using (22)–(24);
Evaluate each krill according to its new location;
Order the krill inhabitants from the most excellent to most unpleasant;
Discover the present most excellent krill individual;
end while
Select the optimal resources associated with the overall best krill;

4. Simulation results

This part simulates the performance of the MSBP-PTS and MSBP-PTS-ORA algorithms using the standard EdgeCloudSim v4.0 and compares their effectiveness with the existing algorithms (e.g., MSBP [14], MORA [18], OppoCWOA [20], MDVMA [22] and COTBIS [23]).

The comparative analysis is prepared in terms of batch sizes, network sustainability range, rate of relocated VMs, overall response time and total cost.

4.1. Simulation setup

In this simulation, the actual 16 fog nodes and 27 edge nodes are used as the trial IoT system structure wherein all nodes are nearby deployed with an edge device i.e., 16 fog servers. Also, the VM migrations are enabled by the optical connection. The edge device is set with the integrated processing ability determined as the number of resource elements. At first, there are n VMs functioning over the network.

Table 2
Edge cloud-sim parameters

Entity type	Parameters	Range
Tasks cloudlets	Task length	1–1500
	Number of tasks	150
	Priority of the tasks	Low, medium and high
VM	Number of VMs	35
	MIPS	500–2000
	VM memory (RAM)	256–2048MB
	Bandwidth	500Mbps–1000Gbps
	Cloudlet scheduler	Space shared and time shared
	Number of PEs requirement	1–4
Data center	Number of datacenter	10
	Number of host	2–5
	VM scheduler	Space shared and time shared

The specifications utilised in the Edge Cloud-Sim are listed in Table 2.

These parameters can be assigned based on the configurations of the system utilized for experiments, i.e. the experiments are conducted on a system equipped with Intel ® Core ™ i5-4210 CPU @ 2.80 GHz, 4GB RAM, 1TB HDD under Windows 10 64-bit operating system. Also, such parameters are adjusted during multiple experiments and the best set of parameters is identified while achieving maximum network efficiency.

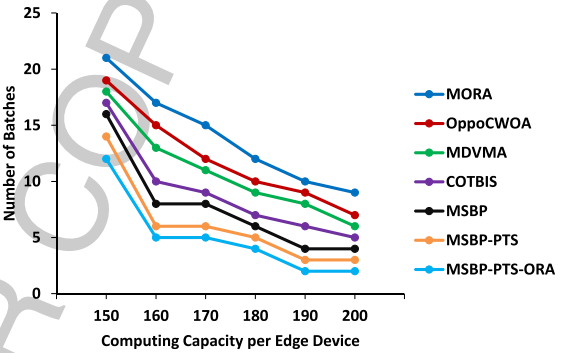

Fig. 2. Number of batches vs. computing capacity per edge device.

4.2. Number of batches

Figure 2 illustrates the number of batches obtained for various task scheduling and RA algorithms under a varying amount of computing capacity per edge device in the edge-cloud paradigm. From this analysis, it is observed that the MSBP-PTS-ORA algorithm has reduced the number of batches compared to the MSBP-PTS and MSBP algorithms due to scheduling the tasks and optimizing the resources effectively. When the computing capacity per edge device is 150, the number of batches for the MSBP-PTS-ORA algorithm is 42.86% less than the MORA, 36.84% less than the OppoCWOA, 33.33% less than the MDVMA, 29.41% less than the COTBIS, 25% less than the MSBP-PTS and 14.29% less than the MSBP algorithms. This is because of optimizing both tasks and resources during VM migration.

4.3. Network sustainability level

Figure 3 depicts as the network sustainability level accomplished by the different task scheduling and RA under varying amount of computing capacity per edge device. From this analysis, it is noticed that the MSBP-PTS-ORA algorithm has an increased level of network sustainability than all other existing algorithms because of reducing the frequent VMs migration by scheduling tasks and optimizing the resources. For example, when the computing capacity per edge device is 150, the network sustainability level of the MSBP-PTS-ORA algorithm is 54.55% higher than the MORA, 41.67% higher than the OppoCWOA, 32.81% higher than the MDVMA, 23.19% higher than the COTBIS, 18.06% higher than the MSBP and 6.25% higher than the MSBP-PTS algorithms.

4.4. Percentage of migrated VMs

Figure 4 illustrates the percentage of migrated VMs for various task scheduling and RA under a varying amount of computing capacity per edge device. From this analysis, found that the MSBP-PTS-ORA algorithm has the lowest percentage of migrated VMs compared to the other algorithms which indicate the MSBP-PTS-ORA reduces the frequent migration of VMs and total computing resource requirement of VMs. For example, when the computing capacity per edge device is 150, the percentage

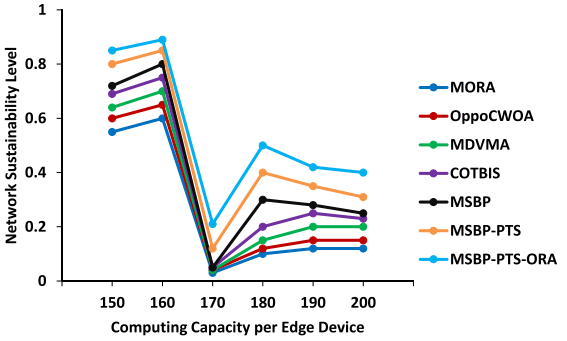

Fig. 3. Network sustainability level vs. computing capacity per edge device.

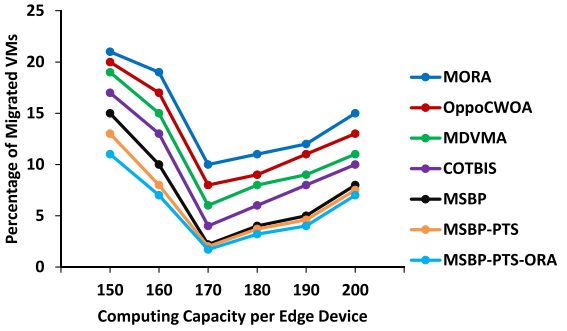

Fig. 4. Percentage of migrated VMs vs. computing capacity per edge device.

of migrated VMs of the MSBP-PTS-ORA algorithm is 47.62% less than the MORA, 45% less than the OppoCWOA, 42.11% less than the MDVMA, 35.29% less than the COTBIS, 26.67% less than the MSBP and 15.38% less than the MSBP-PTS algorithms.

4.5. Overall response time

Figure 5 illustrates the overall mean response period of various task scheduling and RA algorithms. From this analysis, it is observed that the MSBP-PTS-ORA algorithm has minimized overall mean response time associated to the other algorithms due to the prioritized task scheduling and optimal resource distribution during VM migration. The overall mean response time of the MSBP-PTS-ORA algorithm is 24.06% reduced than the MORA, 21.62% reduced than the OppoCWOA, 18.36% reduced than the MDVMA, 14.8% reduced than the COTBIS, 10.55% reduced than the MSBP and 5.06% reduced than the MSBP-PTS algorithms.

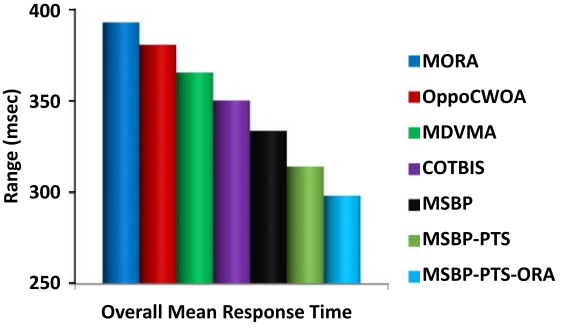

Fig. 5. Comparison of overall average response period.

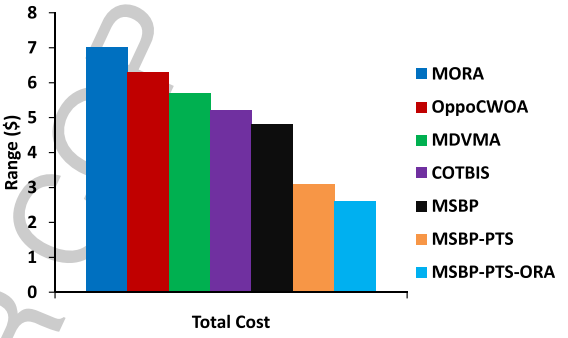

Fig. 6. Comparison of total cost.

4.6. Total cost

The overall cost of fog and cloud servers comprises the processor rate, queue storage, VM memory and system bandwidth.

Figure 6 illustrates the total cost of various task scheduling and RA algorithms. From this analysis, it is noticed that the MSBP-PTS-ORA algorithm has a minimum total cost than the other algorithms due to the minimization of VM migrations efficiently. The total cost of the MSBP-PTS-ORA algorithm is 62.86% less than the MORA, 58.73% less than the OppoCWOA, 54.39% less than the MDVMA, 50% less than the COTBIS, 45.83% less than the MSBP and 16.13% less than the MSBP-PTS algorithms.

The MSBP-PTS-ORA is a realistic and effective approach to achieve optimum task scheduling and RA with least energy use, ease of implementation, and cost compared to the other traditional algorithms used for edge-fog task scheduling and RA, it can be inferred from these studies and results. This approach is utilized for use in cloud data centres as well. Additionally, this MSBP-PTS-ORA can be used as a road plan for putting real-time applications onto RedRIS, Amazon EC2, etc.

5. Conclusion and future work

In this paper, the MSBP-PTS-ORA algorithm was developed for allocating both tasks and resources in fog-cloud computing efficiently. All incoming requests were initially assigned to the nearest fog server and all requests on the fog server were placed in the appropriate priority queue. These requests were then processed and a small number of them were sent to another fog server if the available resources were not sufficient to fulfill the request within the allotted time frame. If the fog layer lacks sufficient resources to fulfill the request, the request was then sent to the cloud. Besides, the KH optimization was applied to allocate the optimal resources during VM migration by solving the NP-hard problem of RA. So, the batch sizes were reduced and the network sustainability was guaranteed while maintaining the provision stability. At last, the simulation results proved that the MSBP-PTS-ORA algorithm has 2 batches, 0.4 network sustainability level and 7% of migrated VMs when the computing capacity per edge device is 200. Also, the MSBP-PTS-ORA algorithm has an overall mean response time of 298.3msec and a total cost of 2.6$ compared to the other MSBP algorithms.

But, the convergence and exploration performance of the KH optimization is not satisfactory when multiple objectives are considered. Because it causes Pareto-issue i.e., the tradeoff issue between the total costs and the network delay. So, future work will focus on adopting advanced optimization algorithms to solve the multi-objective optimization problem for RA.

References

[1] F. Cirillo, F.J. Wu, G. Solmaz and E. Kovacs, Embracing the future internet of things, *Sensors* **19**(2) (2019), 1–20.

[2] M. Majid, S. Habib, A.R. Javed, M. Rizwan, G. Srivastava, T.R. Gadekallu and J.C.W. Lin, Applications of wireless sensor networks and internet of things frameworks in the industry revolution 4.0: a systematic literature review, *Sensors* **22**(6) (2022), 1–36.

[3] S.J. Moore, C.D. Nugent, S. Zhang and I. Cleland, IoT reliability: a review leading to 5 key research directions, *CCF Transactions on Pervasive Computing and Interaction* **2**(3) (2020), 147–163.

[4] T. Alsboui, Y. Qin, R. Hill and Al-H. Aqrabi, Distributed Intelligence in the internet of things: challenges and opportunities, *SN Computer Science* **2**(4) (2021), 1–16.

[5] A. Manimuthu, V. Dharshini, I. Zografopoulos, M.K. Priyan and C. Konstantinou, Contactless technologies for smart cities: big data, IoT, and cloud infrastructures, *SN Computer Science* **2**(4) (2021), 1–24.

[6] P. Sunhare, R.R. Chowdhary and M.K. Chattopadhyay, Internet of things and data mining: an application oriented survey, *Journal of King Saud University-Computer and Information Sciences* **34**(6) (2020), 3569–3590.

[7] M. Noura, M. Atiquzzaman and M. Gaedke, Interoperability in internet of things: taxonomies and open challenges, *Mobile Networks and Applications* **24**(3) (2019), 796–809.

[8] R. Medeiros, S. Fernandes and P.G. Queiroz, Middleware for the internet of things: a systematic literature review, *Journal of Universal Computer Science* **28**(1) (2022), 54–79.

[9] R. Krishnamurthi, A. Kumar, D. Gopinathan, A. Nayyar and B. Qureshi, An overview of IoT sensor data processing, fusion, and analysis techniques, *Sensors* **20**(21) (2020), 1–23.

[10] G. Hatzivasilis, I. Askoxylakis, G. Alexandris, D. Anicic, A. Bröring, V. Kulkarni,... and G. Spanoudakis, The Interoperability of Things: Interoperable solutions as an enabler for IoT and Web 3.0. In *IEEE 23rd International Workshop on Computer Aided Modeling and Design of Communication Links and Networks*, (2018), pp. 1–7.

[11] S. Kumar, P. Tiwari and M. Zymbler, Internet of Things is a revolutionary approach for future technology enhancement: a review, *Journal of Big Data* **6**(1) (2019), 1–21.

[12] I. Ullah, S. Ahmad, F. Mehmood and D. Kim, Cloud based IoT network virtualization for supporting dynamic connectivity among connected devices, *Electronics* **8**(7) (2019), 1–28.

[13] M.F. Manzoor, A. Abid, M.S. Farooq, N.A. Nawaz and U. Farooq, Resource allocation techniques in cloud computing: a review and future directions, *Elektronika ir Elektrotechnika* **26**(6) (2020), 40–51.

[14] W. Hou, W. Li, L. Guo, Y. Sun and X. Cai, Recycling edge devices in sustainable internet of things networks, *IEEE Internet of Things Journal* **4**(5) (2017), 1696–1706.

[15] I.A. Elgendy, W. Zhang, Y.C. Tian and K. Li, Resource allocation and computation offloading with data security for mobile edge computing, *Future Generation Computer Systems* **100** (2019), 531–541.

[16] H. Rafique, M.A. Shah, S.U. Islam, T. Maqsood, S. Khan and C. Maple, A novel bio-inspired hybrid algorithm (NBIHA) for efficient resource management in fog computing, *IEEE Access* **7** (2019), 115760–115773.

[17] Z. Sharif, L.T. Jung, I. Razzak and M. Alazab, Adaptive and Priority-based Resource Allocation for Efficient Resources Utilization in Mobile Edge Computing, *IEEE Internet of Things Journal*, (2021).

[18] A. Araldo, A.D. Stefano and A.D. Stefano, Resource allocation for edge computing with multiple tenant configurations, In *Proceedings of the 35th Annual ACM Symposium on Applied Computing*, (2020), pp. 1190–1199.

[19] S. Tuli, S. Ilager, K. Ramamohanarao and R. Buyya, Dynamic scheduling for stochastic edge-cloud computing environments using a3c learning and residual recurrent neural networks, *IEEE Transactions on Mobile Computing* (2020), 1–15.

[20] Z. Movahedi and B. Defude, An efficient population-based multi-objective task scheduling approach in fog computing systems, *Journal of Cloud Computing* **10**(1) (2021), 1–31.

[21] F. Hoseiny, S. Azizi, M. Shojafar and R. Tafazolli, Joint QoS-aware and cost-efficient task scheduling for fog-cloud resources in a volunteer computing system, *ACM Transactions on Internet Technology* **21**(4) (2021), 1–21.

[22] D. Alsadie, A metaheuristic framework for dynamic virtual machine allocation with optimized task scheduling in cloud data centers, *IEEE Access* **9** (2021), 74218–74233.
[23] R. Rajavel, S.K. Ravichandran, K. Harimoorthy, P. Nagappan and K.R. Gobichettipalayam, IoT-based smart healthcare video surveillance system using edge computing, *Journal of Ambient Intelligence and Humanized Computing* **13**(6) (2022), 3195–3207.
[24] A.S. Abohamama, A. El-Ghamry and E. Hamouda, Real-time task scheduling algorithm for IoT-based applications in the cloud–fog environment, *Journal of Network and Systems Management* **30**(4) (2022), 1–35.
[25] S.K. Panda, S.S. Nanda and S.K. Bhoi, A pair-based task scheduling algorithm for cloud computing environment, *Journal of King Saud University-Computer and Information Sciences* **34**(1) (2022), 1434–1445.

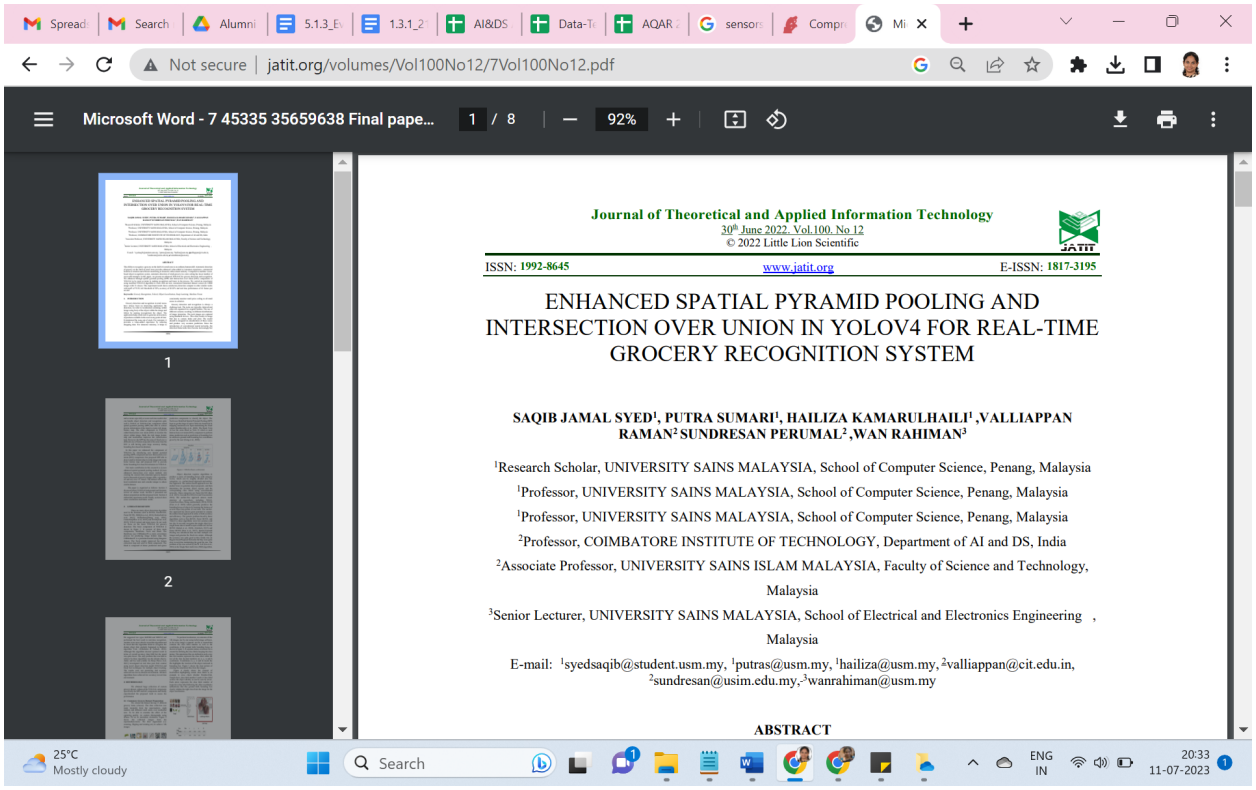
jatit.org/volumes/Vol100No12/7Vol100No12.pdf
Microsoft Word - 7 45335 35659638 Final pape...
1 / 8
92%
Journal of Theoretical and Applied Information Technology
30th June 2022. Vol.100. No 12
© 2022 Little Lion Scientific
ISSN: 1992-8645
www.jatit.org
E-ISSN: 1817-3195
ENHANCED SPATIAL PYRAMID POOLING AND INTERSECTION OVER UNION IN YOLOV4 FOR REAL-TIME GROCERY RECOGNITION SYSTEM
SAQIB JAMAL SYED[1], PUTRA SUMARI[1], HAILIZA KAMARULHAILI[1], VALLIAPPAN RAMAN[2] SUNDRESAN PERUMAL[2], WAN RAHIMAN[3]
[1]Research Scholar, UNIVERSITY SAINS MALAYSIA, School of Computer Science, Penang, Malaysia
[1]Professor, UNIVERSITY SAINS MALAYSIA, School of Computer Science, Penang, Malaysia
[1]Professor, UNIVERSITY SAINS MALAYSIA, School of Computer Science, Penang, Malaysia
[2]Professor, COIMBATORE INSTITUTE OF TECHNOLOGY, Department of AI and DS, India
[2]Associate Professor, UNIVERSITY SAINS ISLAM MALAYSIA, Faculty of Science and Technology, Malaysia
[3]Senior Lecturer, UNIVERSITY SAINS MALAYSIA, School of Electrical and Electronics Engineering , Malaysia
E-mail: [1]syedsaqib@student.usm.my, [1]putras@usm.my, [1]hailiza@usm.my, [2]valliappan@cit.edu.in, [2]sundresan@usim.edu.my,-[3]wanrahiman@usm.my
ABSTRACT
25°C
Mostly cloudy
Search
ENG
IN
20:33
11-07-2023

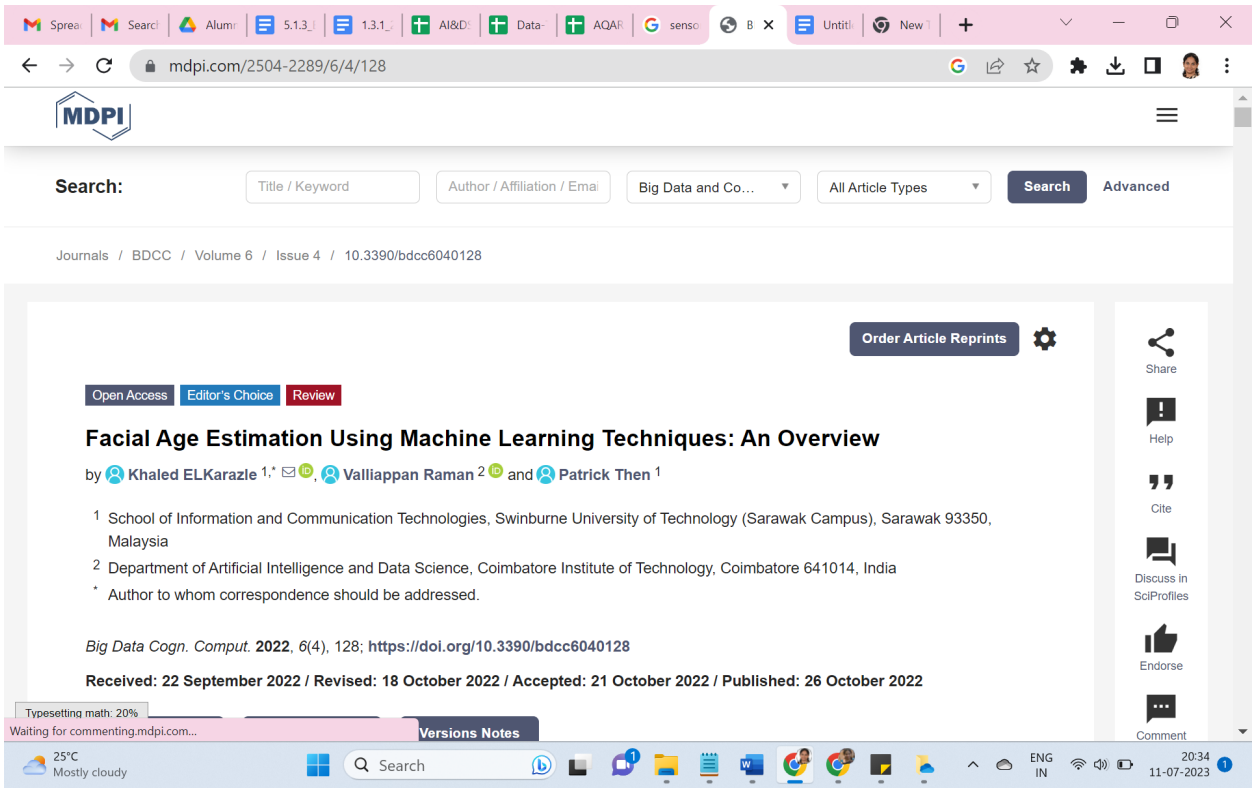
mdpi.com/2504-2289/6/4/128
MDPI
Search:
Title / Keyword
Author / Affiliation / Emai
Big Data and Co...
All Article Types
Search
Advanced
Journals / BDCC / Volume 6 / Issue 4 / 10.3390/bdcc6040128
Order Article Reprints
Share
Help
Cite
Discuss in SciProfiles
Endorse
Comment
Open Access
Editor's Choice
Review
Facial Age Estimation Using Machine Learning Techniques: An Overview
by Khaled ELKarazle [1,*], Valliappan Raman [2] and Patrick Then [1]
[1] School of Information and Communication Technologies, Swinburne University of Technology (Sarawak Campus), Sarawak 93350, Malaysia
[2] Department of Artificial Intelligence and Data Science, Coimbatore Institute of Technology, Coimbatore 641014, India
* Author to whom correspondence should be addressed.
Big Data Cogn. Comput. 2022, 6(4), 128; https://doi.org/10.3390/bdcc6040128
Received: 22 September 2022 / Revised: 18 October 2022 / Accepted: 21 October 2022 / Published: 26 October 2022
Typesetting math: 20%
Waiting for commenting.mdpi.com...
Versions Notes
25°C
Mostly cloudy
Search
ENG
IN
20:34
11-07-2023

thesai.org/Publications/ViewPaper?Volume=13&Issue=9&Code=IJACSA&SerialNo=86

Article Details

Mobile Food Journalling Application with Convolutional Neural Network and Transfer Learning: A Case for Diabetes Management in Malaysia

Author 1: Jason Thomas Chew Author 2: Yakub Sebastian Author 3: Valliapan Raman Author 4: Patrick Hang Hui Then

Digital Object Identifier (DOI) : 10.14569/IJACSA.2022.0130986

DOWNLOAD PDF

Article Published in International Journal of Advanced Computer Science and Applications(IJACSA), Volume 13 Issue 9, 2022.

Abstract and Keywords | How to Cite this Article | {} BibTeX Source

Abstract: Diabetes is an ever worsening problem in modern society, placing a heavy burden on healthcare systems. Due to the association between obesity and diabetes, food journaling mobile applications are an effective approach for managing and improving the outcome of diabetics. Due to the efficacy of nutritional tracking and management in managing diabetes, we implemented a deep learning-based Convolutional Neural Network food classification model to aid with food logging. The model is trained on a subset of the Food-101 and Malaysian Food 11 datasets, including web-scraped images, with a focus on food items found locally in Malaysia. In our experiments, we explore how fine-tuning of the image dataset improves the performance of the model.

Upcoming Conferences

Future of Information and Communication Conference (FICC) 2023

2-3 March 2023 Virtual

Computing Conference 2023

22-23 June 2023

London, United Kingdom

25°C Mostly cloudy Search ENG IN 20:34 11-07-2023

mdpi.com/1424-8220/23/3/1225

MDPI

Order Article Reprints

Open Access Review

Detection of Colorectal Polyps from Colonoscopy Using Machine Learning: A Survey on Modern Techniques

by Khaled ELKarazle [1,*], Valliappan Raman [2], Patrick Then [1] and Caslon Chua [3]

[1] School of Information and Communication Technologies, Swinburne University of Technology, Sarawak Campus, Kuching 93350, Malaysia

[2] Department of Artificial Intelligence and Data Science, Coimbatore Institute of Technology, Coimbatore 641014, India

[3] Department of Computer Science and Software Engineering, Swinburne University of Technology, Melbourne 3122, Australia

* Author to whom correspondence should be addressed.

Sensors **2023**, *23*(3), 1225; **https://doi.org/10.3390/s23031225**

Received: 27 December 2022 / Revised: 8 January 2023 / Accepted: 17 January 2023 / Published: 20 January 2023

(This article belongs to the Section **Sensing and Imaging**)

Download | Browse Figures | Versions Notes

Altmetric Share Help Cite Discuss in SciProfiles Endorse Comment

Waiting for commentingres.mdpi.com...

25°C Mostly cloudy Search ENG IN 20:35 11-07-2023

Hindawi
Journal of Nanomaterials
Volume 2022, Article ID 8270718, 6 pages
https://doi.org/10.1155/2022/8270718

Research Article

Machine Learning-Based Management of Hybrid Energy Storage Systems in e-Vehicles

E. Chandra Blessie,[1] Sharath Kumar Jagnannathan,[2] Brahmadesam Viswanathan Krishna,[3] D. Beulah David,[4] R. Maheswari,[5] M. Pavithra,[6] P. AnanthaChristu Raj,[7] Sivakumar Paramasivam,[8] and Vasireddy Raghu Ram Prasad[9]

[1]*Department of Computing (AI & ML), Coimbatore Institute of Technology, Coimbatore, India*
[2]*Frank J. Guarini School of Business, Saint Peter's University, 2641 John F. Kennedy Boulevard, Jersey City, New Jersey, USA*
[3]*Department of CSE, Rajalakshmi Engineering College, Chennai, India*
[4]*Institute of Information Technology, Saveetha School of Engineering, Thandalam, India*
[5]*HoD-Cyber Physical Systems, Centre for Smart Grid Technologies, SCOPE, Vellore Institute of Technology, Chennai, India*
[6]*Department of CSE, K. Ramakrishnan College of Technology, Samayapuram, India*
[7]*Department of Robotics Engineering, Karunya Institute of Technology and Sciences, Coimbatore, India*
[8]*Department of Mechanical Industrial Engineering, University of Technology and Applied Sciences, Muscat, Oman*
[9]*Faculty of Electrical and Computer Engineering, Arba Minch Institute of Technology, Arba Minch University, Ethiopia*

Correspondence should be addressed to Vasireddy Raghu Ram Prasad; prasad.raghu@amu.edu.et

Received 12 July 2022; Revised 30 July 2022; Accepted 3 August 2022; Published 29 August 2022

Academic Editor: Samson Jerold Samuel Chelladurai

In transportation systems based on e-vehicles, the energy demand is met with the integration of renewable energy sources while maintaining the voltage profile and mitigating the active and reactive power losses. Vehicle-to-grid optimization technique is used to ensure this integration. Minimum active and reactive power losses are achieved when e-vehicles are integrated with the renewable energy sources in a hybrid mode. A machine learning framework with nested learning is used to ensure optimal methodology to trigger vehicular movement and monitoring of the SoC battery level. When the HEV operates, there is a high possibility for battery degradation, leading to loss of its capacity. To determine the optimal policy, the TD(λ) learning algorithm is incorporated. This algorithm is known to showcase high performance and a high convergence rate in a non-Markovian environment. The output is simulated to record the readings observed which is aimed at optimizing the total operation cost and reduction in battery replacement. The results show that for shorter drives, the battery replacement cost is more and it is optimally possible to increase the battery life by 21% using the proposed work. Similarly, the recordings indicate that the proposed work shows a significant reduction of about 8%–10% in the operating cost when compared with the RL and rule-based policy.

1. Introduction

There is a rapid increase in energy demand by consumers across several applications. The voltage profile has to be maintained while reducing the energy losses in order to meet these demands by distribution network operators. Consumers are provided with energy through large distribution and transmission networks from the centralized energy generation power plants. Throughout this process, due to distribution and transmission losses, around 35% electricity is lost. By 2030, the electricity demand is estimated to rise to 900 GW while the environmental pollution may rise to 59% by conventional energy sources that operates towards meeting this demand [1]. In order to meet the demands of

the consumers, renewable energy sources (RESs) are installed close to the load centers.

Along with the distribution and transmission losses, environmental pollution can also be reduced with appropriate integration [2]. At the consumer end, the green energy generation sources installed are termed RESs. Microhydro, wind turbines, solar photovoltaics, and so on are some of the types of RESs [3]. The system complexity increases with high losses, random energy consumption profiles, and different types of connected sources with the integration of the RES. Identification of objectives and integrated approaches are implemented with the integration of the RES. It is crucial to integrate the backup energy sources to increase the reliability of the RES [4]. e-Vehicles or battery stations can be considered as a backup energy source. During transportation, the excess energy from the e-vehicles can be supplied back to the grid, enabling better payoffs at the consumer end [5].

When energy storage facilities are not available, the self-consumption at the generation site increases by 20–40% with the integration of additional devices as the renewable generation and load profiles do not coincide with each other [6]. In Germany, the installation of over 34000 decentralized solar energy storage systems was carried out in the past three years. In the domestic fields, new photovoltaic plants are installed as a routine to enable these applications [7]. During the past few years, despite the availability of several commercial energy storage devices like supercapacitors, chemical-hydrogen storage, and batteries, none of these devices has an efficient tracking and management system. Often, there is a compromise in the energy device as none of the devices can meet all the requirements of the customer for any specific application according to Daniel and Besenhard [8].

The high-power residential storage systems have a high energy density. When two or more energy storage systems are combined together, the coupling benefits the applications as one system complements the other based on the demand. An overall high efficiency is achieved by the management system design in such cases. Improper utilization of the available energy and facilities may result if the renewable energy allocation is not optimized. Hybrid energy storage systems (HESS) are formed by pairing two different storage devices. These devices are paired with each other and operate on a swap mode. It is primarily used in the building sector and several other applications. Coupling HESS with complementary characteristics is beneficial as the strengths of each device complement the other to optimize the system.

Multiple energy storage systems are interchangeably operated by the hybrid system thereby benefiting from the most efficient characteristics of each storage facility. An electric vehicle installed with photovoltaic components consisting of a vanadium redox flow battery as well as a solar lead-acid battery is considered as the HESS in this work. At a smart house premise, the power required to charge the e-vehicle with the integration of the vanadium redox flow battery and the solar lead-acid battery via PV installation is considered to be a commercially mature technology as it meets the load demand in an optimized manner. Low fluctuations are observed when lower grid interactions occur at a higher self-energy consumption rate at both the energy storage systems. This energy is termed the upper target. During deep discharges, intolerance and high current characteristics are observed with short cycle life in the lead-acid battery systems.

The power and capacity of the battery are independent of their sizes, making them easy to differentiate. Without causing any damage to the system, these batteries can perform deep discharge while maintaining the cycle durability of VRB-type batteries. It is possible to operate the battery in higher power ranges by replacing it with a powerful one or by increasing the capacity of the storage tanks. However, when compared to VRB, the lead-acid battery systems have a considerable efficiency rate, medium energy density, shorter reaction time, and financially favorable conditions. When compared to the lead-acid battery systems, the VRB has lesser efficiency and a higher price and can be called an immature technology [9]. Some of the key contributions of this proposed work include the following:

(i) Decrease in the HEV operating cost with respect to battery replacement and fuel cost

(ii) Optimal methodology to trigger vehicular movement and monitoring of the SoC battery level

(iii) Outer-loop adaptive learning to decrease battery replacement costs and inner-loop reinforcement learning to decrease the amount of fuel consumption

2. Literature Survey

In order to reduce the reliance on fossil fuels and adopt RESs, decentralization of electrical energy generation is a crucial step [10]. Over the past few years, there has been a 7% increase in wind power and 4% increase in solar PV globally. There has been a 13% increase in wind energy and 27% increase in the solar PV-based energy generation on average in the last five years [11, 12]. RESs depend on weather constraints and are unpredictable, small in capacity, and complex. In conventional power systems, several issues and challenges with respect to high active and reactive power losses, voltage profile balancing, and network reliability are caused by these characteristics [13, 14]. Hybrid backup energy source models and enhanced integration approaches are used by researchers to analyze the impact of the RES on the system. Some of the most commonly used energy backup sources are the battery banks and e-vehicles. They supply power to the grid during peak and emergency hours and increase reliability due to their interconnections. The system reliability is enhanced by researchers by considering battery banks as backup sources. Very few researchers have paid attention to using e-vehicles for this purpose. While overcoming the electric constraints, integration of e-vehicles into the grid is crucial.

Reliability assessment and the advantages of integration of the RES are discussed in [15]. Reference [16] discusses the integration approaches and challenges of distribution of energy sources and the uncertainty model. For energy

management, [17] discusses distributed energy resource optimization using an internet framework. Reference [18] discusses and analyzes the issues of unbalanced grids and voltage sag. The case studies with implementation in Western Australia, architecture development and application, and adaptive schemes for renewable energy source integration are discussed in [17] for overcoming the issues in the optimization of the RES. Improving the distribution network voltage profile, minimization of the utility cost, energy generation cost, tariff structuring, initial cost, carbon emission, line loading, real and reactive power losses, and other such multiple advantages rely on the proper allocation of the RES. Machine learning, neural network, particle swarm optimization, genetic algorithms, fuzzy logic controller, and other tools can be used for the optimization of voltage sensitivity analysis, voltage indexing, power loss sensitivity techniques, and other novel methods used for RES integration. In order to integrate the RES into the grid, the roadmap is discussed by the authors in [19] whereas the limitations of integration of the RES into the grid are discussed by the authors in [20]. Various optimization techniques for the integration of e-vehicles and the grid are discussed by the authors of [21]. The reliability of the RES and integrated grid can be improved largely by identifying an appropriate vehicle-to-grid optimization approach.

The currently used HESS systems cannot be optimized with conventional techniques. Several researchers are exploring and researching the control systems for this reason. The energy flow between the conventional battery and supercapacitor is managed with rule-based algorithms in Chatzakis et al. [22]. The threshold values are compared for parameters like battery output current and load demand for the application of the respective rule. The lithium-ion battery and LAB are used for the constitution of the HESS, which is controlled using the abovementioned techniques. The results are compared by Piao et al. [23]. When compared to first-order filtering, the rule-based approach termed "amplitude sharing algorithm" delivers better results. When the battery and fuel cell or battery and superconducting magnet are used as power storage systems, the power allocation is managed efficiently with the help of a fuzzy logic controller as observed in Zhang et al. [24] and Min et al. [25].

Without the need for complex mathematical knowledge, the most appropriate alternative can be chosen from the set of rules designed by experts using the rule-based algorithms to which this control technique belongs. With the increase in complexity of the system, the difficulty in configuration also increases [26]. The current technique in Zhang et al. [24] focuses on the smooth operation of fuel cells rather than the exploitation of storage systems with high-efficiency operation ranges. The generalization of the setting and attribution of a group of rules prior to design the management techniques for the analyzed HESS is weakened and is not considered within the scope of this paper. The first-order filtering technique is the commonly used HESS management technique in the existing literature. A conventional battery system is used in addition to a supercapacitor or any other storage system to manage the high power fluctuations according to this technique [22, 27]. Along with several parameters, the response time of the two energy storage systems is considered for designing the linear filtering system.

In the current management system, the design is independent of the response time, and hence, the filtering techniques presented by Changhao et al. and Liu et al. [23, 27] are unsuitable. Shema et al. [28] analyze a HESS project on the Pellworm island of the North Sea. Cost-efficient and stable energy supply is achieved by exploiting the redox flow batteries and lithium-ion batteries used in the storage system of the renewable energy sources, namely, 300 kWp wind farm and 700 kWp PV park. The optimization approach can follow the mixed-integer linear programming technique. The generalization part is not available in the linear programming algorithms that are applicable in a simple and easily comprehensive manner. When global solutions are claimed, this approach can be avoided. Hybrid techniques are often preferred in the existing literature as several techniques are combined thereby overcoming several drawbacks. For example, two neural networks are combined with a low-pass filter by Xia et al. in [29] to decide the reference power percentage that must be allocated to each facility. The efficiency behavior is worsened by the excessive on-site generation or demand energy partitioning between the available storage devices, making this technique unfavorable. As explained, unlike the case designed here, low pass filters are not applied. Chatzakis et al. in [22] conceptualized the combination of a filtering technique with a rule-based algorithm. However, the requirements mentioned in this topic cannot be fulfilled by this system.

3. Proposed Architecture

The proposed work is aimed at decreasing the HEV operating cost with respect to battery replacement and fuel cost. A machine learning framework with nested learning is used to ensure optimal methodology to trigger vehicular movement and monitoring of the SoC battery level. Here, an outer-loop adaptive learning to decrease battery replacement costs and inner-loop reinforcement learning to decrease the amount of fuel consumed are incorporated. In the inner loop reinforcement learning is used because of the following considerations:

(1) The HEV energy management inner loop holds information on the current fuel consumption, power demand, and vehicle speed without retaining any prior information on the vehicle parameters

(2) Different HEV operation modes are required to change the battery charge level, power demand, and change in vehicle speed for a driving trip. Based on the current state, different actions are taken using a reinforcement learning agent

(3) Instead of decreasing the instantaneous fuel consumption at every time step, the inner-loop HEV energy management focuses on decreasing the total amount of fuel consumed during the driving trip. Similarly, instead of the immediate reward, reinforcement learning targets the cumulative return optimization

For optimal energy management, knowledge on the current reward and current state of the system is required, without need for prior information. To decrease fuel usage, SoH degradation in the battery is taken into consideration along such that the inner-loop reinforcement learning involves battery capacity fading. The system works such that the inner loop acts as an independent HEV energy management system that automatically decreases the operating cost. To determine the optimal SoC range, an adaptive learning methodology is used in the outer loop for several trips. The SoH battery degradation can be identified by observing the SoC range. Hence, the outer loop is important in decreasing battery replacement in the e-vehicle. Moreover, using prior information about the average speed and trip length during the driving trip, it is possible to reduce the battery replacement cost, by the outer loop.

3.1. SoH Estimation. When the HEV operates, there is a high possibility for battery degradation, leading to loss of its capacity. In general, a battery is said to reach its life expectancy when its fading level reaches 20%–30%. This can be expressed as follows:

$$Q_{\text{fade}} = \frac{1 - Q_{\text{full}}}{Q_{\text{full}}^{\text{nom}}} \times 100\%, \tag{1}$$

such that Q_{full} represents the full charge capacity of the battery and $Q_{\text{full}}^{\text{nom}}$ is the nominal value of Q_{fade}.

Similarly, the state of charge (SoC) can be expressed using equation (2) as follows:

$$\text{SoC} = \frac{Q_{\text{batt}}}{Q_{\text{full}}} \times 100\%. \tag{2}$$

On continuous operation, the total capacity fading after M cycles can be determined using equation (3) as follows:

$$Q_{\text{fade}} = \sum_{m=1}^{M} Q_{\text{fade,cycle}}(m). \tag{3}$$

It has been observed that the charging/discharging cycle of the battery holds the same average SoC and same SoC swing. But, in practical scenarios, it is not possible for the battery to adhere to a specific charging/discharging cycle pattern. Hence, a cycle-decoupling methodology which can be used to determine the pattern of battery charging/discharging is used. Using this technique, it is possible to calculate the total fading capacity of the battery.

3.2. Reinforcement Learning. In the reinforcement learning environment, "agent" represents the decision maker while every other thing is known as the "environment." An agent-environment interaction is represented in Figure 1 for a sequence of "t" discrete time steps. Here, the state of the environment is observed for every step "t" such that a set of possible actions and states is taken into consideration. After one time step, the outcome of the action taken is given as a reward while a new state is established in a different

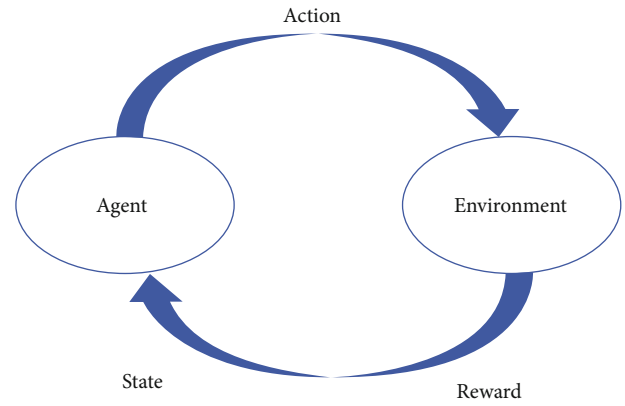

Figure 1: Interaction between the agent and the environment.

Table 1: Key parameters.

Denotation	Parameters	Rating
L_w	Distance between wheels and axles	2.5 m
A	Vehicle frontal area	3.48 m^2
M	Total vehicle mass	1360 kg
η	Total transmission efficiency	98%
R_w	Wheel radius	0.36 m
f_e	Bearing friction coefficient	0.001
α	Total gear ratio	10.0

environment. To incorporate inner-loop reinforcement learning, the reward for the action taken should be known to the HEV controller (agent) as it plays a crucial part in deriving the optimal policy. For an action taken "a" in state "s," the reward "r" can be evaluated using the following formula:

$$r = -m_f.\Delta T - w.\Delta Q_{\text{fade}}, \tag{4}$$

such that w represents the battery weight, xx is the length of the time step, and ΔQ_{fade} and w are the battery capacity fading and fuel consumption rate, respectively. Here, $m_f.\Delta T$ can be determined directly from the fuel consumption while ΔQ_{fade} can be determined with the help of SoH estimation and cannot be determined online. However, since the time complexity is large, it is safer to derive ΔQ_{fade} using an equivalent cycle method.

Accordingly, it is possible to calculate the SoQ_{avg} and $\text{SoQ}_{\text{swing}}$ values using equation (5) as follows:

$$\begin{aligned} \text{SoQ}_{\text{high}} &= \max_t \text{SoQ}(t), \\ \text{SoQ}_{\text{low}} &= \min_t \text{SoQ}(t), \\ \text{SoQ}_{\text{avg}} &= \frac{\text{SoQ}_{\text{high}} + \text{SoQ}_{\text{low}}}{2}, \\ \text{SoC}_{\text{swing}} &= \text{SoQ}_{\text{high}} - \text{SoQ}_{\text{low}}. \end{aligned} \tag{5}$$

Table 2: Operating cost of the proposed, RL, and rule-based policies.

Trip	Distance	Proposed (in Rs.)	RL (in Rs.)	Rule-based (in Rs.)
Gandhipuram to Brookfield Road	3 km	Rs.4.26 per unit	Rs.4.52 per unit	Rs.4.64 per unit
Gandhipuram to Sai Baba Colony	2.7 km	Rs.4.06 per unit	Rs.4.36 per unit	Rs.4.58 per unit
Gandhipuram to Rs. Puram	2.9 km	Rs.4.12 per unit	Rs.4.46 per unit	Rs.4.65 per unit
Saravanampatti to Ganapathy	4 km	Rs.5.45 per unit	Rs.5.69 per unit	Rs.5.83 per unit
Saravanampatti to Gandhipuram	8.7 km	Rs. 12.64 per unit	Rs.14.04 per unit	Rs. 15.12 per unit

3.3. TD(λ) Learning Algorithm. To determine the optimal policy, the TD(λ) learning algorithm is incorporated. This algorithm is known to showcase high performance and a high convergence rate in a non-Markovian environment. The lambda "λ" parameter represents the trace decay parameter. It lies within the range 0 and 1. Here, for every state-action pair, the Q value is represented by $Q(s, a)$. The charge level is represented as "q" and the vehicle speed is represented as "v" with respect to the state "s." Similarly, the action "a" will pick the kth gear ratio and its corresponding "i" current is discharged from the battery. The following are the steps involved in the TD(λ) algorithm:

Step 1. An arbitrary value is assigned for $Q(s, a)$ at the initial stage.

Step 2. For every step "t," an action "a" is chosen based on the values of $Q(s, a)$.

Step 3. The exploration-exploitation policy is used to avoid the risk of being caught in an optimal solution. This means that for the current state, the maximum $Q(s, a)$ is not chosen using the action "a".

Step 4. Based on the action chosen, a new state is identified and given the reward.

Step 5. According to the reward and state, the values of $Q(s, a)$ are updated for the various values of (s, a) pairs within $e(s, a)$. $e(s, a)$ represents the eligibility of every state-action pair that has been previously used.

Step 6. A new constant λ is used which holds a value between 0 and 1.

Step 7. When using the eligibility of the state-action pair, it is not necessary to update "e" and the Q value for every state action.

Step 8. Hence, a record of the most recent state-pair action "M" is recorded while all other pairs are ignored.

4. Result and Discussion

The operation of the electric vehicle is simulated and developed using vehicle simulator ADVISOR. Table 1 represents the key parameters that are taken into consideration. In this work, we have compared the proposed work with the rule-based policy and reinforcement learning policy.

The output is recorded. Based on the simulation results observed, the following are the outcomes recorded:

(1) On optimizing the total operation cost, it is seen that the replacement cost of the battery is significant

(2) The cost of replacing the battery is a significant part of the total operating cost and is even identified to be higher than the fuel cost

(3) The RL policy that is in effect will use the rule-based policy to decrease the fuel consumption. However, this policy will not take into consideration the cost of the battery

The results of the observations are tabulated in Table 2 which also shows that for shorter drives, the battery replacement cost is more and it is optimally possible to increase the battery life using the proposed work.

The reading was taken for several trips across Coimbatore, Tamil Nadu, India, and the amount of charge required for the trips was recorded. The recordings indicate that the proposed work was able to record a significant reduction in the operating cost when compared with the RL and rule-based policy.

5. Conclusions and Future Scope

In this paper, the HEV energy management is outlined as well as a solution to efficiently manage it through optimization of the HEV operating cost with respect to battery replacement and fuel cost. In this work, the instantaneous fuel consumption is decreased at every time step, with focus on reducing the total amount of fuel consumed with inner-loop HEV energy management. Similarly, instead of the immediate reward, reinforcement learning targets the cumulative return optimization. The proposed work indicates that for shorter drives, the battery replacement cost is more and it is optimally possible to increase the battery life by 21%. The readings observed also show significant reduction of about 8%–10% in the operating cost when compared with the RL and rule-based policy.

Data Availability

The data used to support the findings of this study are included within the article.

Conflicts of Interest

The authors declare that there are no conflicts of interest regarding the publication of this paper.

References

[1] A. Talwariya, P. Singh, and M. L. Kolhe, "Stackelberg game theory based energy management systems in the presence of renewable energy sources," *IETE Journal of Research*, vol. 67, no. 5, pp. 611–619, 2021.

[2] Y. Xu, Y. Zheng, and Y. Yang, "On the movement simulations of electric vehicles: a behavioral model-based approach," *Applied Energy*, vol. 283, article 116356, 2021.

[3] T. Wang, H. Luo, X. Zeng, Z. Yu, A. Liu, and A. K. Sangaiah, "Mobility based trust evaluation for heterogeneous electric vehicles network in smart cities," *IEEE Transactions on Intelligent Transportation Systems*, vol. 22, pp. 1797–1806, 2020.

[4] Y. Zhang, J. Wang, and Z. Li, "Uncertainty modeling of distributed energy resources: techniques and challenges," *Current Sustainable/Renewable Energy Reports*, vol. 6, no. 2, pp. 42–51, 2019.

[5] S. P. Burger and M. Luke, "Business models for distributed energy resources: a review and empirical analysis," *Energy Policy*, vol. 109, pp. 230–248, 2017.

[6] J. Weniger, T. Tjaden, and V. Quaschning, *Solare Unabhängigkeitserklärung*, Photovoltaik, 2012.

[7] K. P. Kairies, D. Haberschusz, J. Jonas van Ouwerkerk et al., *JahresberichtzumSpeichermonitoringentstandimRahmen des ForschungsvorhabensWissenschaftliches Mess¬ und EvaluierungsprogrammSolarstromspeicher (WMEP PV¬Speicher)*, InstitutfürStromrichtertechnik und ElektrischeAntriebe der RWTH, Aachen, 2016.

[8] C. Daniel and J. O. Besenhard, *Handbook of Battery Materials*, Wiley-VCH Verlag GmbH & Co. KGaA, Weinheim, Germany, 2 edition, 2011.

[9] L. Baumann, *Improved System Models for Building-Integrated Hybrid Renewable Energy Systems with Advanced Storage: A Combined Experimental and Simulation Approach*, PhD Thesis, De Montfort University, Leicester, UK, 2015.

[10] E. Paglia and C. Parker, "The intergovernmental panel on climate change: Guardian of climate science," in *Guardians of Public Value*, pp. 295–321, Palgrave Macmillan, Cham, Switzerland, 2021.

[11] W. He, L. Tao, L. Han, Y. Sun, P. E. Campana, and J. Yan, "Optimal analysis of a hybrid renewable power system for a remote island," *Renewable Energy*, vol. 179, pp. 96–104, 2021.

[12] A. Boretti and S. Castelletto, "Cost and performance of CSP and PV plants of capacity above 100 MW operating in the United States of America," *Renewable Energy Focus*, vol. 39, pp. 90–98, 2021.

[13] O. Alves, L. Calado, R. M. Panizio, M. Gonçalves, E. Monteiro, and P. Brito, "Techno-economic study for a gasification plant processing residues of sewage sludge and solid recovered fuels," *Waste Management*, vol. 131, pp. 148–162, 2021.

[14] A. Alsharif, C. W. Tan, R. Ayop, A. Dobi, and K. Y. Lau, "A comprehensive review of energy management strategy in vehicle-to-grid technology integrated with renewable energy sources," *Sustainable Energy Technologies and Assessments*, vol. 47, article 101439, 2021.

[15] B. Huang, A. G. Meijssen, J. A. Annema, and Z. Lukszo, "Are electric vehicle drivers willing to participate in vehicle-to-grid contracts? A context-dependent stated choice experiment," *Energy Policy*, vol. 156, article 112410, 2021.

[16] O. Ouramdane, E. Elbouchikhi, Y. Amirat, and E. S. Gooya, "Optimal sizing and energy management of microgrids with vehicle-to-grid technology: a critical review and future trends," *Energies*, vol. 14, no. 14, p. 4166, 2021.

[17] A. Rolán, S. Bogarra, and M. Bakkar, "Integration of distributed energy resources to unbalanced grids under voltage sags with grid code compliance," *IEEE Transactions on Smart Grid*, vol. 13, no. 1, pp. 355–366, 2021.

[18] W. Hadingham, K. Rayney, A. Blaver, B. Smart, and J. Thomas, "Distributed energy resources roadmap: how the state of Western Australia is leading in integration," *IEEE Power and Energy Magazine*, vol. 19, no. 5, pp. 76–88, 2021.

[19] A. Talwariya, P. Singh, and M. Kolhe, "A stepwise power tariff model with game theory based on Monte-Carlo simulation and its applications for household, agricultural, commercial and industrial consumers," *International Journal of Electrical Power & Energy Systems*, vol. 111, pp. 14–24, 2019.

[20] M. P. Lalitha, V. C. V. Reddy, and N. S. Reddy, "Application of fuzzy and ABC algorithm for DER placement for minimum loss in radial distribution system," *Iranian Journal of Electrical and Electronic Engineering*, vol. 6, no. 4, pp. 248–257, 2010.

[21] A. Kumawat, R. Choudhary, and P. Singh, "Optimal placement of DER and capacitor for minimizing the power losses using genetic algorithm," *International Research Journal of Engineering and Technology (IRJET)*, vol. 2, no. 3, pp. 2306–2309, 2015.

[22] J. Chatzakis, K. Kalaitzakis, N. C. Voulgaris, and S. N. Manias, "Designing a new generalized battery management system," *IEEE Transactions on Industrial Electronics*, vol. 50, no. 5, pp. 990–999, 2003.

[23] C. Piao, Q. Liu, Z. Huang, and X. Shu, "VRLA battery management system based on LIN bus for electric vehicle," in *Advanced Technology in Teaching*, vol. 163, pp. 753–763, AISC.

[24] Z. Cheng-Ning, Z. Zheng, Z. Ca-Iping, and Z. Yupu, "Design on dispersed management system for traction battery pack in electric transmission vehicle," *Acta Armamentarii*, vol. 28, no. 4, pp. 396–398, 2017.

[25] M. Luo, Y. Xiao, W.-M. Sun, and Z. Wang, "Online battery monitoring system based on GPRS for electric vehicles," in *2013 5th International Conference on Intelligent Human-Machine Systems and Cybernetics*, Hangzhou, China, August 2013.

[26] M. Lelie, T. Braun, M. Knips et al., "Battery management system hardware concepts: an overview," *Applied Sciences*, vol. 8, no. 4, p. 534, 2018.

[27] L. Xiaokang, Z. Qionghua, H. Kui, and S. Yuehong, "Battery management system for electric vehicles," *Huazhong University of Science & Technology (Nature Science Edition)*, vol. 35, no. 8, pp. 83–86, 2017.

[28] S. A. Mathew, R. Prakash, and P. C. John, "A smart wireless battery monitoring system for electric vehicles," in *2012 12th International Conference on Intelligent Systems Design and Applications (ISDA)*, Kochi, India, November 2012.

[29] X. Zezhong, S. Hongliang, and L. Ting, "Remote monitoring system of lead-acid battery group based on GPRS," in *2010 International Conference on Electrical and Control Engineering*, Wuhan, China, June 2010.

JOURNAL PUBLICATION PROOF

PERIOD- JUNE 2022-MAY 2023

Faculty: Dr.J.Shana

Journal: YMER, July 2022

JUXTAPOSITION BETWEEN TWO CONVOLUTIONAL NEURAL NETWORK FOR MUSIC GENRE CLASSIFICATION

[1] Dr. J. Shana, [2] Ms. N. Priyadharshini Jayadurga, [3] Pratiba K R, [4] Prakash R
[1,2,3,4] *Department of Computing – Artificial Intelligence and Machine Learning,*
[1,2,3,4] *Coimbatore Institute of Technology, Coimbatore*
[1] *shana@cit.edu.in,* [2] *dharshinidurga@cit.edu.in,* [3] *pratiba.karthi@gmail.com,*
[4] *prakashr7d@gmail.com*

ABSTRACT

Music genre classification is the fundamental step involved in building a strong recommendation system. If music classification has to be carried out manually, then one has to listen to numerous songs and then select the genre. This process is not only time-consuming, it is quite a tedious task. The music industry has seen an excellent flow of latest channels to browse and distribute music. This doesn't return without drawbacks. With the increase in data, manual curation has become a difficult task. Audio files have a plethora of features that could be used to make parts of this process a lot easier. Advancements in technology have made it possible to extract the features of audio files. However, the most effective way to handle these for various tasks is unknown. This paper compared the two deep learning models of convolutional neural networks namely Alex-net and Res-net for the purpose of music genre classification using mel-spectrogram images for training. These aforementioned models were tested on GTZAN datasets. It was found that the results showed 56.0% accuracy for the res-net model which was outperformed by alex-net with an accuracy of 80.5%.

Keywords: *GTZAN Dataset, Alex-net, Res-net, Convolutional Neural Network*

INTRODUCTION

With the increase in technology, the amount of data being available to the public is increasing day by day. The increase of data is rapid to the point where manual curation is becoming infeasible and classification using automated systems are necessary. The music industry is no exception. Automating the process of music tagging would end in higher organization of the information and thereby creating any further development on the data is easier, like making themed playlists or recommending songs to users.

Machine learning is used to find the delicate patterns within the data, which might preferably be tough to explicitly code algorithms for. One such case is deciding what genre a song belongs to, that is the use case this report can cover. Companies (such as Soundcloud, Apple Music, Spotify, Wynk etc) use music classification, either to place recommendations to their customers, or simply as a product (like Shazam). Automatic musical genre classification can assist humans or perhaps replace them in this process and would be of a very valuable addition to music information